Cell

Tel2 Regulates the Stability of PI3K-Related Protein Kinases

Hiroyuki Takai,[1] Richard C. Wang,[1,3] Kaori K. Takai,[1] Haijuan Yang,[2] and Titia de Lange[1,*]
[1]Laboratory for Cell Biology and Genetics, The Rockefeller University, 1230 York Avenue, New York, NY 10065, USA
[2]Structural Biology Program, Sloan-Kettering Institute, Memorial Sloan-Kettering Cancer Center, New York, NY 10065, USA
[3]Present address: Department of Dermatology, The University of Texas Southwestern Medical Center at Dallas, 5323 Harry Hines Boulevard, Dallas, TX 75390, USA.
*Correspondence: delange@rockefeller.edu
DOI 10.1016/j.cell.2007.10.052

SUMMARY

We report an unexpected role for Tel2 in the expression of all mammalian phosphatidylinositol 3-kinase-related protein kinases (PIKKs). Although Tel2 was identified as a budding yeast gene required for the telomere length maintenance, we found no obvious telomeric function for mammalian Tel2. Targeted gene deletion showed that mouse *Tel2* is essential in embryonic development, embryonic stem (ES) cells, and embryonic fibroblasts. Conditional deletion of *Tel2* from embryonic fibroblasts compromised their response to IR and UV, diminishing the activation of checkpoint kinases and their downstream effectors. The effects of *Tel2* deletion correlated with significantly reduced protein levels for the PI3K-related kinases ataxia telangiectasia mutated (ATM), ATM and Rad3 related (ATR), DNA-dependent protein kinase catalytic subunit ataxia (DNA-PKcs). *Tel2* deletion also elicited specific depletion of the mammalian target of rapamycin (mTOR), suppressor with morphological effect on genitalia 1 (SMG1), and transformation/transcription domain-associated protein (TRRAP), and curbed mTOR signaling, indicating that Tel2 affects all six mammalian PIKKs. While Tel2 deletion did not alter PIKK mRNA levels, in vivo pulse labeling experiments showed that Tel2 controls the stability of ATM and mTOR. Each of the PIKK family members associated with Tel2 in vivo and in vitro experiments indicated that Tel2 binds to part of the HEAT repeat segments of ATM and mTOR. These data identify Tel2 as a highly conserved regulator of PIKK stability.

INTRODUCTION

PI3K-related protein kinases are key signal transducers that inform eukaryotic cells on their nutrient supply and the status of their genome and its transcripts (Abraham, 2001; Bakkenist and Kastan, 2004; Guertin and Sabatini, 2005; Wullschleger et al., 2006). They phosphorylate target proteins on serine or threonine residues using a C-terminal region related to the catalytic domain of PI3 kinase (Lavin et al., 1995). The kinase domains of the PIKKs are flanked by conserved FAT and FATC domains (Bosotti et al., 2000), and their N termini carry long arrays of HEAT or Armadillo repeats (Andrade and Bork, 1995; Perry and Kleckner, 2003). Mammals have six PIKKs: taxia telangiectasia mutated (ATM), ATM and Rad3 related (ATR), DNA-dependent protein kinase catalytic subunit ataxia (DNA-PKcs), mammalian target of rapamycin, previously FRAP (mTOR), suppressor with morphological effect on genitalia 1 (SMG1), and the catalytically inactive transformation/transcription domain-associated protein (TRRAP). The PIKKs interact with numerous proteins, but none of their binding partners or target proteins is held in common by all family members.

The human PIKKs regulate a diverse set of signaling pathways that are relevant to human health and contribute to the suppression of tumorigenesis. ATM and ATR govern the response to genome damage by phosphorylating key substrates involved in DNA repair and cell-cycle control (Abraham, 2001; Kastan and Bartek, 2004; Shiloh, 2003). ATM is crucial for the response to DNA double-strand breaks (DSBs), whereas ATR is activated by replication stress and certain DNA repair intermediates. Mutations in ATM cause ataxia telangiectasia, while a mutation in ATR results in Seckel syndrome. DNA-PKcs promotes nonhomologous end joining and the diminished V(D)J recombination resulting from DNA-PKcs deficiency is responsible for severe combined immunodeficiency (SCID) in mice. SMG1 is required for the nonsense-mediated decay (NMD) mRNA surveillance pathway (Conti and Izaurralde, 2005). TRRAP is involved in the regulation of

gene expression as a component of histone acetyltransferase complexes (Herceg and Wang, 2005). The sixth mammalian PIKK, mTOR, integrates environmental cues, mitogenic signals, and nutrient availability to control cell growth (Hay and Sonenberg, 2004). The PI3K-AKT-mTOR signaling pathway is frequently altered in human cancer (Shaw and Cantley, 2006; Sabatini, 2006).

Here we report a link between all six mammalian PIKKs and Tel2 (official gene symbol TELO2, also referred to as hCLK2), the mammalian ortholog of the budding yeast TEL2 gene. Along with TEL1, TEL2 was identified in the first screen for yeast mutants with altered telomere length (Lustig and Petes, 1986). Cells that harbor mutant alleles of *tel1* or *tel2* undergo telomere attrition for ~150 generations but ultimately maintain their telomeres at a stable short length. Gene cloning revealed that TEL1 is the budding yeast ortholog of ATM (Greenwell et al., 1995; Morrow et al., 1995). TEL2 was found to be an essential gene, but the TEL2 ORF lacked obvious conserved motifs that might suggest a molecular function (Runge and Zakian, 1996). The conservation of TEL2 in *Drosophila melanogaster* suggested that its function may not be limited to telomere maintenance, since *Drosophila* and other dipterans lack the canonical telomerase-based telomere system (Pimpinelli, 2005). Hypomorphic alleles of the *C. elegans* TEL2 ortholog (Clk-2/Rad-5) show pleiotropic phenotypes, including an extended life span (Lakowski and Hekimi, 1996) and hypersensitivity to DNA damage (Hartman and Herman, 1982) but no significant telomere-length changes. Recent reports have suggested a role for human and fission yeast Tel2 in the response to replication stress (Jiang et al., 2003; Collis et al., 2007; Shikata et al., 2007). We have used gene targeting in mouse cells to determine the function of Tel2 and show that it controls the stability of all PIKKs proteins, thus potentially explaining the pleiotropic nature of the phenotypes of Tel2 mutations.

RESULTS

No Obvious Telomeric Function for Mammalian Tel2

Guided by the work on budding yeast Tel2, we initially explored the possibility that the human and mouse Tel2 orthologs might have telomere-related functions (Figure S1). Using Flag-tagged human Tel2 (Figures 1A and 1B), we asked whether Tel2 can localize to chromosome ends. Indirect immunofluorescence (IF) showed that ectopically expressed Tel2 localized in both the cytoplasm and nucleus (Figure S1C), in agreement with the absence of canonical subcellular localization signals from the Tel2 ORF. However, IF and ChIP analysis failed to provide evidence for a telomeric localization of either ectopically expressed Tel2 or the endogenous protein (Figures S1C–S1E). In addition, shRNA knockdown of Tel2 or overexpression of full-length Tel2 or truncated Tel2 had no significant effect on telomere-length homeostasis in human tumor cell lines or the shortening rate of telomeres in primary human fibroblasts (data not shown). Finally, cells with diminished Tel2 did not show accumulation of 53BP1 or γ-H2AX at their telomeres (data not shown), which is a hallmark of telomere deprotection (Takai et al., 2003). Although these results did not exclude a function for Tel2 at telomeres, they raised the possibility that Tel2 might have other functions in mammalian cells.

Tel2 Is Essential for Embryonic Development and Cellular Growth

To address the function of Tel2, we used targeted gene deletion in the mouse. Mouse Tel2 mRNA appeared to be ubiquitously expressed (Figure S1F) and encodes an ORF starting in the second exon that predicts a 840 aa protein with a molecular weight (MW) of 93 kDa. Our targeting strategy deleted the third exon of the Tel2 gene (Figures 1A and 1B), resulting in a shift in the reading frame at amino acid (aa) 116 into a non-Tel2 ORF that terminates 52 amino acids downstream. Heterozygous $Tel2^{DEL/+}$ mice were viable, fertile, and healthy, suggesting that the truncated protein is either not expressed or has no deleterious effects. Mouse embryonic fibroblasts (MEFs) prepared from $Tel2^{DEL/+}$ embryos grew normally and showed the expected 2-fold reduction in Tel2 protein levels (Figure 1C). Consistent with the lethality of Tel2 deficiency in yeast and *C. elegans* (Benard et al., 2001; Runge and Zakian, 1996; Shikata et al., 2007), the Tel2 null mutation (*DEL/DEL*) caused embryonic lethality (Figure 1D). Tel2 also appeared to be essential in ES cells (Figure S2). When double-targeted $Tel2^{TARGET/FLOX}$ ES cells carrying two conditional Tel2 alleles were treated with Cre to induce Tel2 deficiency, the cells arrested (Figures S2A–S2D), and we were unable to isolate Tel2 null clones from $Tel2^{TARGET/FLOX}$ ES cell cultures in which Cre was expressed (Figure S2E).

To study the cellular consequence of Tel2 deficiency, we prepared $Tel2^{DEL/FLOX}$ MEFs from which Tel2 could be deleted by transduction of a self-deleting Cre retrovirus (H&R Cre) (Silver and Livingston, 2001; Celli and de Lange, 2005) or by 4-hydroxytamoxifen (4-OHT) induction of a Cre-ER fusion protein expressed from the GT(ROSA)26-Sor locus (R26Cre-ER) (Feil et al., 1996; Badea et al., 2003). Expression of Cre recombinase using either system removed the floxed allele efficiently (Figures 2A and 4D and see below). Tel2 protein became undetectable by 4 days after H&R Cre infection of the $Tel2^{DEL/FLOX}$ MEFs (Figure 2A). Similarly, the Tel2 protein disappeared within 2 to 3 days after induction of R26Cre-ER with OHT (see below, Figure 4E). Cells lacking the *Tel2* gene initially grew normally but arrested after 3 to 4 days with a 2N or 4N DNA content, reduced S and M phase index, and a flattened senescence-like morphology (Figures 2B–2E, S3A, and S3B and data not shown). This cell-cycle arrest phenotype was due to loss of Tel2 since ectopic expression of either mouse or human Tel2 cDNA rescued the growth defect (Figures 2C, 2D, S3A, and S3B).

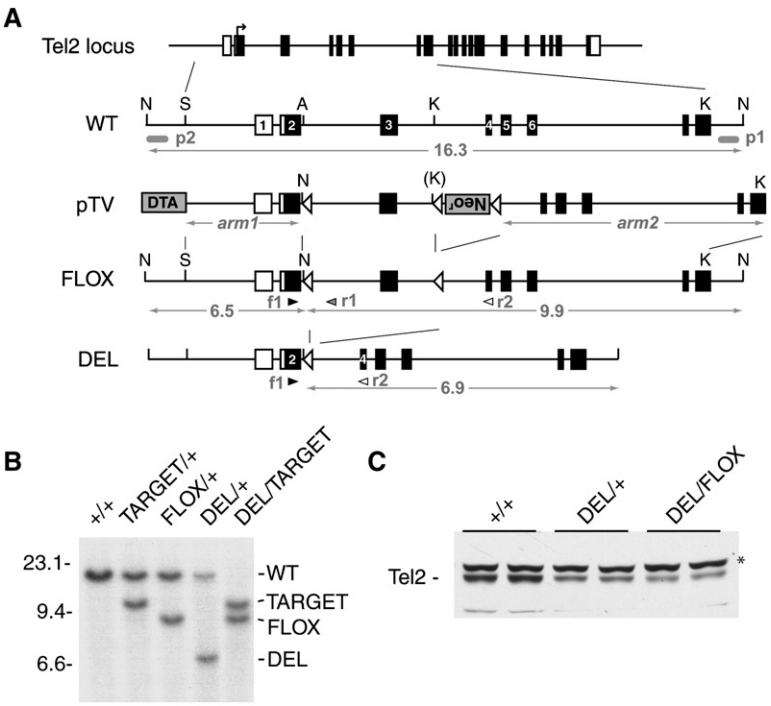

D

Age	+/+	DEL/+	DEL/DEL	ND	Total
E13.5	16	26	0	0	42
3 weeks	23	57	0	2	82

Figure 1. Conditional Deletion of Mouse *Tel2*

(A) Schematic of the mouse Tel2 locus (WT, *Tel2*$^{+}$), the targeting vector (pTV), the conditional allele (*Tel2*^{FLOX}), and the null allele (*Tel2*^{DEL}). *Nde*I fragment sizes are indicated for each genotype, and the probes p1 and p2 are shown. f1, r1, and r2, primers for genomic PCR; N, *Nde*I; S, *Sca*I; K, KpnI; A, *Apa*I.

(B) Genomic blots of ES clones. Genomic DNA digested with *Nde*I and probed with p1. The targeted ES clones were transiently transfected with Cre to generate ES cells harboring the indicated genotypes.

(C) Western blot of Tel2 from MEFs of the indicated genotypes. *, nonspecific signal detected by anti-Tel2 Ab #1039.

(D) Table of the genotypes found in the offspring of heterozygous intercrosses of *Tel2*$^{DEL/+}$ mice at E13.5 and at weaning. The genotype was ambiguous for two embryos (ND).

Tel2 Null Cells Show Diminished DNA-Damage Signaling

The cell-cycle arrest of Tel2-deficient cells did not appear to be due to a DNA-damage response since the nuclei did not contain DNA-damage foci (data not shown) and the phenotype was not affected by abrogation of the p53 pathway (Figure 2B). The arrest was also not accompanied by induction of CDK inhibitors such as p21, p27, and p16 (Figure 3A). There was also no evidence for upregulation of p53, consistent with the lack of p21 induction upon Tel2 deletion.

Interestingly, in cells lacking Tel2, the basal level of phosphorylation of p53 on serine 18 was diminished, and the steady-state levels of p53 and p21 were slightly but reproducibly reduced (Figure 3A). As this reduction in basal p53 activation could be explained if the Tel2-deficient cells had a diminished response to intrinsic DNA damage, we tested their ability to respond to exogenously induced genotoxic stress. Whereas control cells showed the expected IR-induced phosphorylation of Chk2 and a concomitant increase in p53 serine 18 phosphorylation, Tel2-deficient cells failed to show this response and also lacked the ability to upregulate p21 after IR (Figure 3B). These results suggested that the slight reductions in p53 and p21 were due to diminished Chk2 signaling in the Tel2 null cells. Interestingly, the cells were also defective in the induction of Chk1 phosphorylation after UV treatment (Figure 3C), suggesting that Tel2-deficient cells might be generally compromised in their ability to respond to DNA damage. Whereas Tel2 deficiency affected the DNA-damage signaling pathways, IR-induced DNA damage did not appear to alter the localization of human or mouse Tel2 (Figure S1G and data not shown) nor did IR affect the migration of mouse Tel2 protein in SDS/PAGE (Figure 3B and data not shown).

Tel2 Affects PIKK Protein Levels

To further address the effect of Tel2 on the DNA-damage response, we evaluated the status of the ATM kinase in Tel2-deficient cells. Immunoblots revealed that the deletion of Tel2 resulted in a striking reduction in abundance of ATM protein (Figure 4A). Quantification of the data indicated that the residual ATM levels were less than 10% of the controls (data not shown). The lowered abundance of ATM protein was a specific consequence of Tel2 deletion, since the effect was negated by expression of mouse Tel2 from a retroviral vector (Figure 4B). Whereas ATM levels depended on Tel2, the converse was not the case: *Atm*$^{-/-}$ MEFs had normal Tel2 levels (Figure 4C).

The diminished Chk1 phosphorylation in UV-treated Tel2-deficient cells (Figure 3C) suggested that Tel2 might

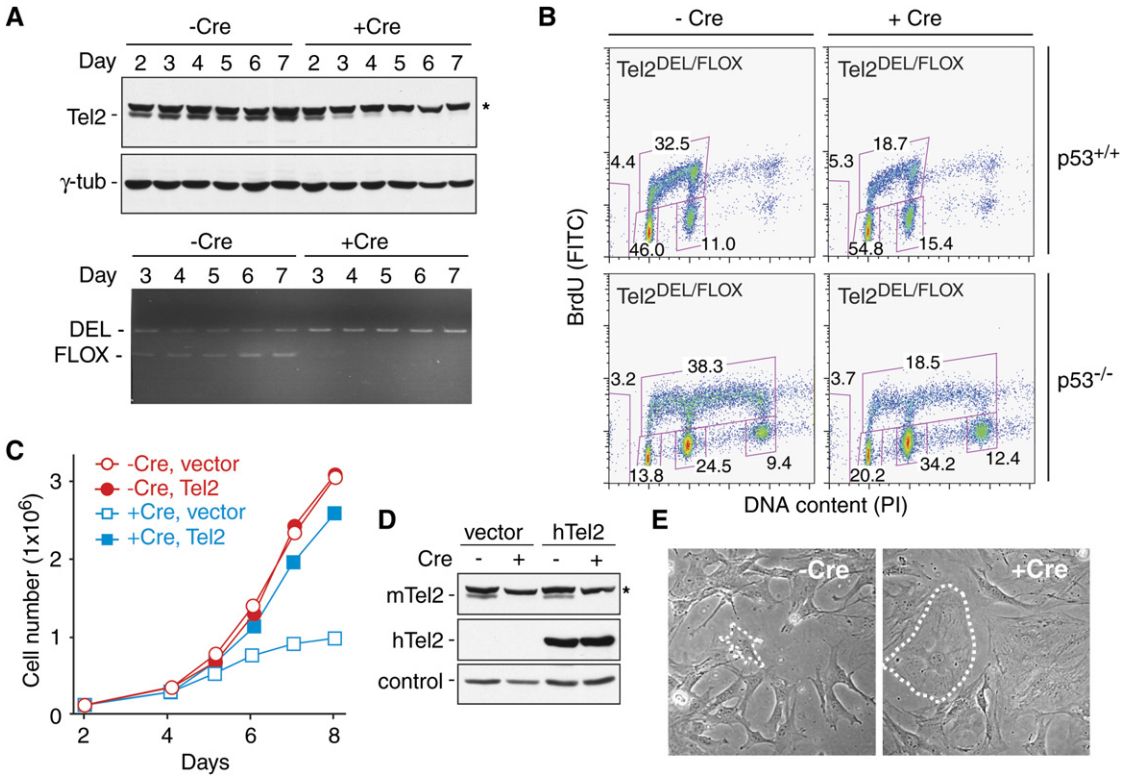

Figure 2. *Tel2* Depletion Results in Cell-Cycle Arrest

(A) Immunoblot for mouse Tel2 protein from $Tel2^{DEL/FLOX}$ MEFs (top) and PCR analysis of genomic DNA isolated from $Tel2^{DEL/FLOX}$ (bottom) at the indicated time points after introduction of Cre with the H&R retrovirus. *, nonspecific signal detected by the anti-Tel2 Ab #1039.

(B) Cell-cycle profile after deletion of Tel2 from $p53^{+/+}$ or $p53^{-/-}$ MEFs. MEFs were infected with H&R Cre (or a mock treatment) and 5 ($p53^{+/+}$) or 6 ($p53^{-/-}$) days later incubated with BrdU for 1 hr, fixed, and analyzed by FACS for DNA (propidium iodide) and BrdU content.

(C) Graph of the growth curves of $Tel2^{DEL/FLOX}$ $p53^{-/-}$ MEFs after H&R Cre infection or mock infection (-Cre). Cells indicated as Tel2 were infected with an hTel2 retrovirus and selected with puromycin before the H&R Cre infection.

(D) Immunoblots for Tel2 in the MEFs used in (C). *, nonspecific signal. control, nonspecific signals detected by the Tel2C antibody.

(E) Phase-contrast micrographs of $Tel2^{DEL/FLOX}$ $p53^{-/-}$ MEFs at day 9 after infection with H&R Cre. The dotted white line highlights a cell with senescent morphology.

also affect the ATR kinase. Indeed, the steady-state level of ATR was strongly diminished upon deletion of Tel2 using the R26Cre-ER system (Figures 4D and 4E). The effect of Tel2 on ATM and ATR was specific since Rif1, a large protein with HEAT repeats involved in the DNA-damage response (Xu and Blackburn, 2004; Silverman et al., 2004) was not affected by Tel2 deletion (Figures 4A and S4A). Moreover, the levels of eight other proteins (Smc1, Rent1, MCM2, NBS1, PTEN, PCNA, PARP, Raptor) were not affected by Tel2 deletion (Figure S4A).

We next queried the other four mammalian PIKKs: mTOR, DNA-PKcs, SMG1, and TRRAP. Each of these PIKKs were affected showing significantly diminished abundance in cells lacking Tel2 (Figure 4E). Quantitative immunoblotting indicated that mTOR, DNA-PKcs, and SMG1 were reduced to ~20% of the control cells (data not shown). The kinetics by which ATM, mTOR, and DNA-PKcs dissipated was similar, whereas the response was somewhat slower for ATR, SMG1, and TRRAP (Figure 4E). As expected, the reduction in mTOR expression affected the signaling by this PIKK as evident from the reduced phosphorylation of the mTOR target p70-S6K on Thr389 (Figures 4F and 4G). Thus, Tel2 deletion from MEFs had a specific effect on the abundance of all mammalian PIKKs with functional consequences for at least three of the PIKK signaling pathways.

We used several other approaches to confirm the effect of Tel2 depletion on the steady-state level of PIKKs. First, we used an shRNA-mediated knockdown system in mouse ES cells that allowed reduction of Tel2 expression through a doxycyclin-inducible shRNA (Figure 4H and I) (Seibler et al., 2007). In these cells, the effect of Tel2 loss on the expression of the ATM and mTOR kinases was confirmed. The ES clone shTel2#4 showed the strongest Tel2 knockdown and the greatest loss of ATM and mTOR protein (Figure 4I and data not shown), suggesting that the reduction in the levels of these two PIKKs correlated with the efficiency of Tel2 depletion. Furthermore, shRNA-mediated knockdown of human Tel2 in hTERT-immortalized BJ fibroblasts resulted in lowered levels of the ATM

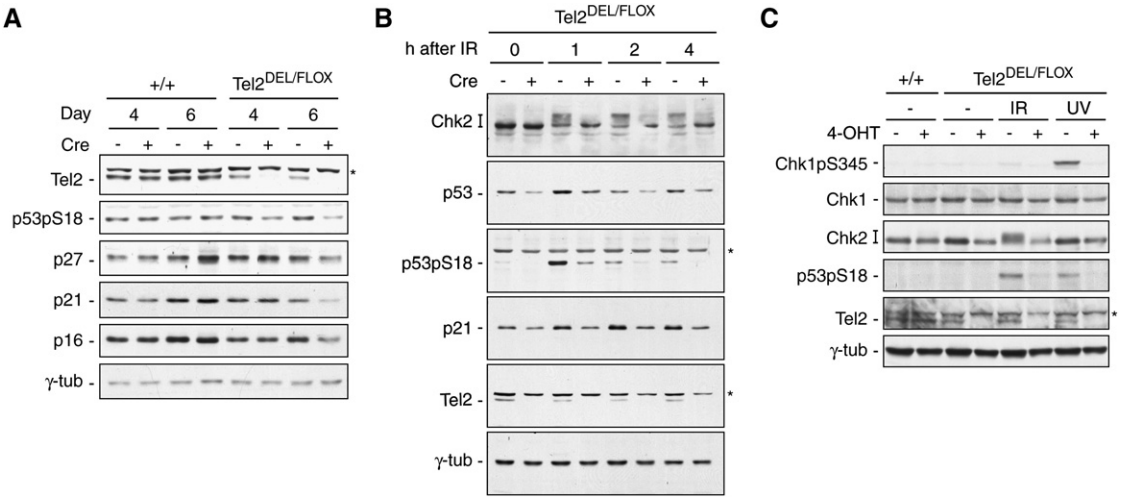

Figure 3. Defective DNA-Damage Response in Cells Lacking *Tel2*

(A) Immunoblots of the indicated MEFs at day 4 and 6 after H&R Cre retrovirus infection.

(B) Immunoblots of time course of the indicated proteins from MEFs treated with IR. Cells were irradiated at day 5 after infection with H&R Cre. *, nonspecific signals.

(C) Immunoblots of extracts prepared from UV and IR-treated MEFs. Cells were treated with or without 2 Gy of γ-irradiation or 25 J/m^2 of UV at day 4 of Cre induction by OHT and cultured for 30 min or 1 hr, respectively.

kinase, indicating that Tel2 controls PIKK expression in human cells as well (Figure 4J).

Finally, we determined whether the observed depletion of the PIKK proteins was a secondary effect of changes in the cell cycle progression of Tel2-deficient cells. One observation arguing against this possibility is that in MEFs the reduction in ATM levels was already evident at day 3 after Tel2 deletion (Figure 4E), at which time the cultures still proliferate at the same rate as the controls (Figure 2C and data not shown). When Tel2-deficient cells stop proliferating, they show diminished entry into S phase and arrest with a 2N- and 4N-DNA content (Figure 2B). We therefore asked whether the lowered PIKK levels could be explained from reduced progression through S phase by examining the levels of ATM and mTOR in quiescent cells. However, human fibroblasts that were arrested in G0 through contact inhibition or serum starvation showed no reduction in ATM and mTOR protein levels (Figure S4B).

Tel2 Affects the Stability of ATM and mTOR

In order to determine the mechanism whereby Tel2 controls the expression of the PIKKs, we examined the effect of Tel2 deficiency on PIKK mRNA levels. Northern blotting revealed that Tel2 deletion did not significantly alter the abundance of the mRNAs for ATM, DNA-PKcs, mTOR, ATR, SMG1, or TRRAP over a period of up to 5 days after deletion of Tel2 (Figure 5A). Additional analysis using other probes to detect the mRNAs and semiquantitative RT-PCR for ATM confirmed that the reduced PIKK levels after Tel2 deletion were not due to lowered mRNA levels (Figure S5 and data not shown).

To test whether Tel2 affected the synthesis or stability of the ATM and mTOR kinases, cells were pulse labeled with ^{35}S-methionine and -cysteine and protein extracts were harvested at various time points after a chase with unlabeled amino acids (Figure 5B). The ATM and mTOR kinases were isolated by immunoprecipitation, and their abundance was quantified by autoradiography. Consistent with the largely unaltered mRNA levels, both ATM and mTOR were synthesized at close to normal rates. Three days after Cre treatment, the incorporation of labeled amino acids into ATM and mTOR was 70% and 90% of control cells, respectively. A 260 kDa control protein in the ATM IPs showed a similar reduction in synthesis rate in Tel2-deficient cells (80% of the rate in wild-type control cells). This minor decrease is most likely due to diminished protein synthesis associated with the depletion of mTOR.

Tel2 had a profound effect on the stability of ATM and mTOR. In Tel2-proficient control cells, the half-lives of ATM and mTOR were approximately 8 and 18 hr, respectively. In contrast, in the Tel2-depleted cells the half-lives of ATM and mTOR were drastically reduced to 1.5 and 2 hr, respectively (Figures 5C and 5D). As a control, we determined the half-life of the 260 kDa protein in the ATM IPs, which was 4 hr in both the control cells and Tel2-deficient cells. Together the results suggested that the reduction of PIKK protein level was primarily due to the destabilization of PIKKs in absence of Tel2. Treatment of cells with the proteasome inhibitors MG-132 and lactacystin did not increase the levels of the PIKKs in Tel2-deficient cells (Figures S6A–S6C), and we have not been able to detect ubiquitylated intermediates. Future experiments will have to address

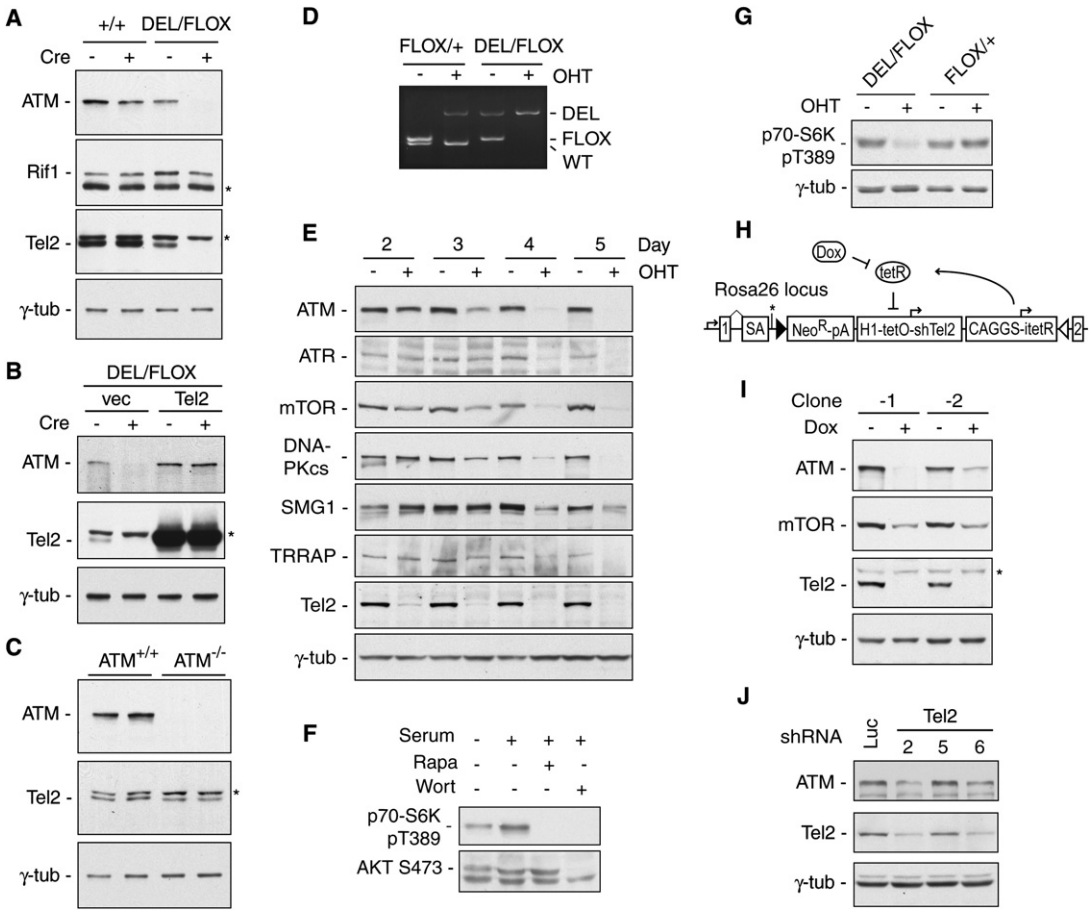

Figure 4. Reduced PIKK Protein Levels upon Tel2 Deletion

(A) *Tel2*$^{+/+}$ and *Tel2*$^{DEL/FLOX}$ MEFs were infected with H&R-Cre retrovirus and harvested after 4 days for immunoblot analysis of the indicated proteins. *, nonspecific bands.

(B) Immunoblots of *Tel2*$^{DEL/FLOX}$ MEFs expressing mouse Tel2 treated with H&R Cre. The indicated proteins were analyzed at day 5 after Cre treatment.

(C) Immunoblotting for Tel2 in *Atm*$^{+/+}$ and *Atm*$^{-/-}$ MEFs.

(D) PCR for conversion of the FLOX allele to the DEL allele by R26Cre-ER induced by OHT; analysis at day 2 after OHT treatment. Cells were p53 deficient.

(E) Time course of PIKK expression in Tel2-depleted MEFs. *Tel2*$^{DEL/FLOX}$ MEFs were treated with 0.5 μM OHT for 6 hr to induce R26Cre-ER, and lysates were prepared at the indicated times. Parallel control cultures were treated identically except for OHT treatment. Tel2 was detected with a mouse polyclonal anti-Tel2 antibody.

(F) Verification of reagents used to query mTOR signaling. Immunoblot for the indicated protein phosphorylation in wild-type MEFs treated with or without 20 nM rapamycin or 200 nM wortmannin. Cells were cultured in 0.5% serum medium for 16 hr. Rapamycin or wortmannin was added 30 min prior to serum stimulation.

(G) Tel2 deletion diminishes mTOR signaling. Immunoblot to determine the phosphorylation of mTOR targets (as in F) in MEFs of the indicated genotypes at 3 days after with or without OHT treatment to induce Cre.

(H) Schematic of the inducible Tel2 shRNA Rosa26 cassette in ES cells. SA, splicing acceptor; pA, poly A sequence; H1, promoter; tetO, tet-operator; CAGGS, promoter; tetR, tet repressor; Dox, doxycycline; *, ATG; open triangle, FRT sequence; closed triangle, FRT F3 sequence.

(I) Tel2 shRNA in ES cells diminishes ATM and mTOR. Tel2 shRNAs were induced with doxycycline in ES cells with the Rosa26 cassette shown in (F), and cells were harvested after 4 days.

(J) Immunoblot for effect of Tel2 knockdown on ATM in human cells. Human BJ-hTERT fibroblasts were infected with the indicated shRNA retroviruses and subjected to puromycin selection for 3 days. *, nonspecific signal.

the degradation pathway of the PIKKs in Tel2-deficient cells.

We considered the possibility that Tel2 might behave like a (co)chaperone for the PIKKs and therefore asked whether Tel2 deletion resulted in mislocalization and/or aggregation of its client proteins. IF analysis did not reveal an altered subcellular distribution of the residual ATM and mTOR in Tel2-deficient cells, and there was no indication of aberrant protein aggregation (Figure S7A). We also tested whether the effect of Tel2 deletion was similar to

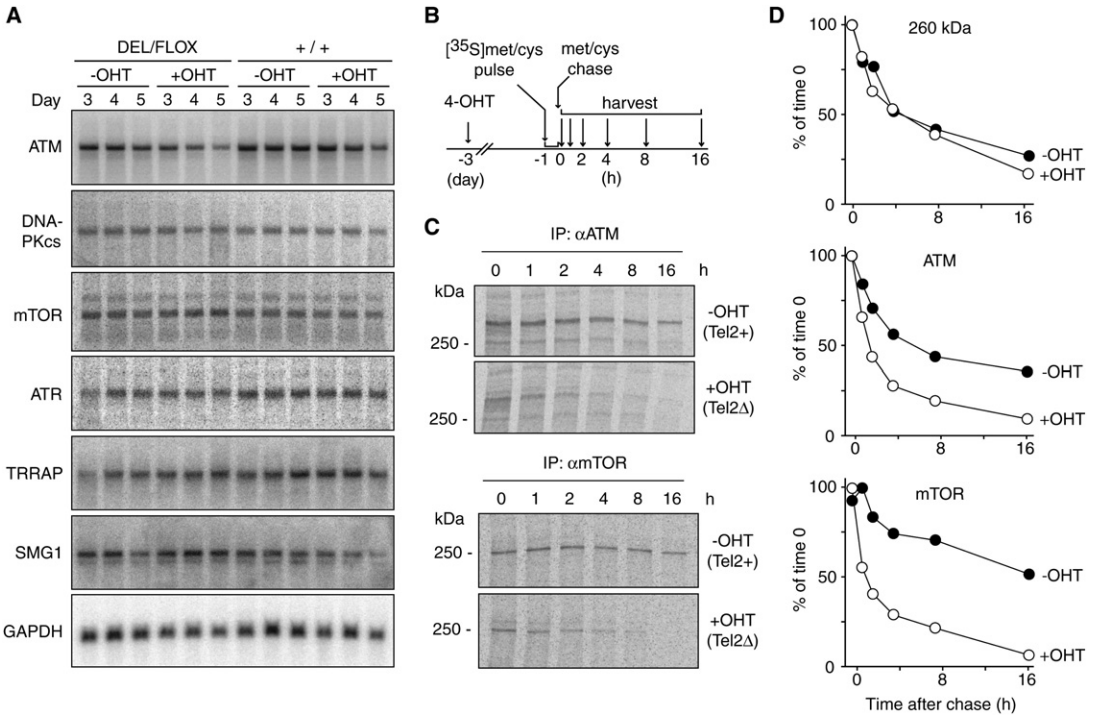

Figure 5. Tel2 Affects PIKK Proteins, Not mRNAs

(A) Northern blots on total RNA from MEFs with the indicated genotypes. Cells were treated with 0.5 μM OHT for 5 hr to deplete Tel2 and harvested at the indicated time points. Control cells were treated similarly except for OHT treatment.

(B) Experimental timeline for protein stability studies. *Tel2*$^{DEL/FLOX}$ MEFs were treated with 0.5 μM OHT for 6 hr to deplete Tel2 and cultured for 3 days in normal medium. The cells were pulse labeled with ^{35}[S]-methionine and -cysteine for 1 hr (horizontal bar) and then chased with media containing cold met/cys for the indicate time periods before harvesting protein extracts.

(C) Analysis of ATM and mTOR protein stability. Lysates prepared at the indicated times were subjected to immunoprecipitation with anti-ATM and-mTOR antibodies. Radio-labeled ATM and mTOR were detected by autoradiography of SDS-PAGE gels.

(D) Quantitative analysis of the data shown in (C). The 260 kDa internal control protein is an unidentified protein recovered in the ATM IPs.

that of geldanamycin, an inhibitor of Hsp90. Although ATM and DNA-PKcs levels were diminished upon treatment with the geldanamycin analog 17-AAG, neither mTOR nor SMG1 were affected (Figure S7B). Since the effects of 17-AAG and Tel2 deletion are distinct, we consider it unlikely that Tel2 acts as an Hsp90 cochaperone.

Tel2-PIKK Interactions

As Tel2 affected the stability of ATM and mTOR and presumably the other PIKKs, we examined the possibility that Tel2 might be associated with these proteins. Mass spectrometric analysis revealed that Tel2 is associated with at least two PIKKs. A dual Flag- and $[HA]_2$-tagged Tel2 protein (FH_2-Tel2) was expressed in HeLa S3 cells and sequentially immunoprecipitated using anti-Flag and anti-HA antibody conjugated beads followed by MALDI-TOF mass spectrometric analysis of associated proteins. This analysis revealed DNA-PKcs and ATR in the Tel2 complex (Figure 6A). ATR was also identified as a Tel2-associated protein by Boulton and colleagues (Collis et al., 2007). Immunoblotting analysis showed that ATM, mTOR, and SMG1 were also present in the Tel2 complex derived from HeLa cells (Figure 6B), although their abundance was too low for their detection by MALDI-TOF. A number of control proteins, including Chk2 and PARP1, and several shelterin components were not recovered in association with Flag-Tel2 (Figure 6B and data not shown). The interaction between Tel2 and the PIKKs was also detected for the endogenous proteins (Figure 6C). Endogenous human ATM, ATR, DNA-PKcs, mTOR, and TRRAP were recovered in IPs of the endogenous Tel2 but not in the IP of a control protein (TRF1) (Figure 6C). As an additional negative control, we found that PI3K-γ was not recovered with Tel2. Tel2 also did not show a detectable association with several PIKK-interacting proteins. We were unable to detect ATRIP, Nbs1, or Raptor in the Tel2 IPs (Figure 6C and data not shown), and the expression of Raptor and Nbs1 were unaffected by Tel2 deletion (Figure S4A). Finally, we confirmed the interaction between Tel2 and the PIKKs in mouse cells. Endogenous mouse mTOR and ATM could be coimmunoprecipitated with myc-tagged Tel2 expressed in MEFs, whereas a control protein (MCM2) was not recovered (Figure 6D). MEFs infected with the empty vector served as a control and showed that the recovery of mTOR and ATM in the myc IPs is dependent on Tel2

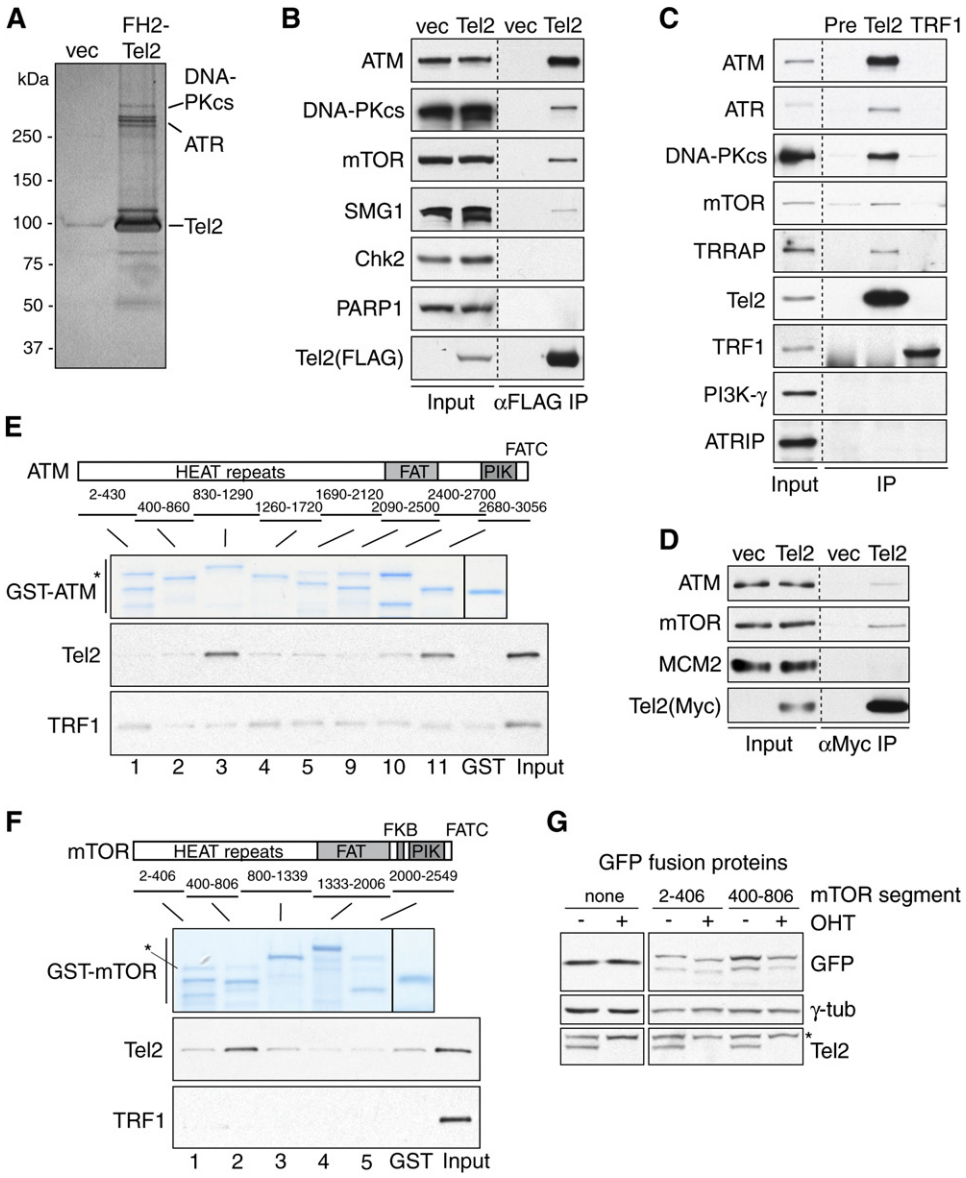

Figure 6. Tel2 Interacts with All Mammalian PIKKs and Binds HEAT-Repeat Segments of mTOR and ATM

(A) Silver-stained gel of a Tel2 complex isolated by FLAG/HA affinity purification of an N-terminally tagged FLAG-$[HA]_2$-Tel2 construct expressed in the human HeLa S3 clone. DNA-PKcs and ATR were identified based on 23 and 7 peptide sequences, respectively.

(B) Immunoblots showing specific association of Tel2 with all mammalian PIKKs. Tel2 was isolated as in (A) and queried for associated proteins by immunoblotting.

(C) Association of endogenous Tel2 with PIKKs. Extract prepared form HeLa S3 cells was used for the immunoprecipitation with Tel2C, preimmune serum, or TRF1 antibody. IPs were analyzed by immunoblotting for the indicated proteins.

(D) Immunoblot analysis of the association of mouse Tel2 with ATM and mTOR. N-terminal Myc-tagged hTel2 expressed in MEFs was affinity purified using anti-Myc beads and queried for the indicated associated proteins.

(E) Tel2 binds to HEAT repeat and C-terminal regions of ATM. Equal amounts of purified bacterially expressed GST-ATM fusion proteins (top) and GST alone were incubated with purified baculovirus-derived Tel2 or TRF1, bound to glutathione beads, and washed. Bound proteins were eluted and visualized by immunoblotting using Tel2B (middle) or TRF1 371 antibodies (bottom). *, nonspecific peptide purified with GST fusion proteins.

(F) Tel2 binds to a HEAT-repeat segment of mTOR. Equal amounts of purified GST-mTOR fusion proteins (top) were treated as described in (E). *, nonspecific peptide copurified with GST fusion proteins.

(G) Tel2-mediated stabilization conferred onto GFP by the HEAT-repeat fragment of mTOR. GFP or GFP fused to the indicated segments of mTOR (see panel F) were expressed in *Tel2*$^{DEL/FLOX}$ MEFs, and Cre was induced with OHT. After 4 days, the levels of Tel2 and the GFP fusion proteins was determined by immunoblotting as shown.

expression. Collectively, these results indicate that Tel2 can interact with each of the six mammalian PIKKs.

Since our mass spectrometry analysis did not reveal potential factors that might mediate the interaction of Tel2 with the PIKKs, we set out to determine whether Tel2 can bind PIKKs directly. Fragments of the ATM kinase were fused to GST and used to pull down Tel2 produced in insect cells (Figure 6E). TRF1 served as a negative control. Tel2 bound to a fragment representing the middle of the HEAT-repeat region (aa 830–1290) as well as to a fragment from the C terminus of ATM representing the kinase domain and the FATC region (aa 2680–3056). Tel2 also bound to a portion of HEAT-repeat region of mTOR (aa 400–806) but did not show a specific interaction with the kinase domain or the FATC region of mTOR (Figure 6F). The ability of Tel2 to bind mTOR directly was further verified by examining the interaction of proteins produced in insect cells (Figure S8). When tagged Tel2 and mTOR were coexpressed in insect cells, a complex containing Tel2 and mTOR could be isolated using the tags for either Tel2 or mTOR indicating a direct interaction. Raptor did not appear to interfere with the binding of Tel2 to mTOR. These data suggest that Tel2 binds directly to HEAT-repeat segments in the N terminus of mTOR and ATM. The interaction appears specific since Tel2 did not bind to six other HEAT-repeat fusion fragments tested (Figures 6E and 6F), and Tel2 did not appear to interact with PI3K-γ, which also contains HEAT repeats (Figure 6C). HEAT repeats occur in the N terminus of each of the six mammalian PIKKs and are conserved aspects of PIKKs in other eukaryotes, raising the possibility that Tel2 binds to each of the PIKKs through an interaction with a subset of the HEAT repeats.

To determine whether the Tel2-binding fragment of mTOR could confer Tel2-dependent stability onto a different protein, GFP was fused to aa 400–806 of mTOR or to aa 2–406, which served as a negative control. GFP and the two GFP fusion proteins were introduced into *Tel2*$^{DEL/FLOX}$ MEFs, and their abundance was determined by western blotting before and after deletion of Tel2. The results showed that while GFP itself and the fusion of GFP to the HEAT repeats in aa 2–406 of mTOR were unaffected by Tel2 deletion, the abudance of the GFP fusion containing the Tel2-binding site of mTOR was significantly diminished in Tel2-deficient cells. We note that while this mTOR-GFP fusion protein was clearly affected by Tel2 status, the reduction in its expression level was less prominent than the endogenous full-length mTOR. Therefore it is possible that the stabilization of mTOR by Tel2 involves regions outside aa 400–806.

DISCUSSION

PIKKs are eukaryotic signal transducers that govern pathways of major relevance to human disease. Our results reveal that the six mammalian PIKKs (ATM, ATR, DNA-PKcs, SMG1, mTOR, and TRRAP) share Tel2 as an interacting partner and regulator. In the absence of Tel2, the steady-state level of all PIKKs is drastically reduced and the signaling pathways governed by ATM, ATR, and mTOR are curtailed. Tel2 binds to a site in the HEAT-repeat regions of ATM and mTOR and prevents their rapid degradation, and we assume that binding of Tel2 to the other PIKKs similarly affects their stability.

The role of Tel2 as a stabilizer of PIKKs could potentially explain why Tel2 is essential in eukaryotes, including in mice, as we show here for mouse embryos, MEFs, and ES cells. Drastically lowered levels of one or more essential PIKKs can explain why Tel2 is essential in mouse cells and embryos. Although mice lacking some PIKKs (e.g., ATM and DNA-PKcs) are viable, deficiency in mTOR, ATR, and TRRAP results in early embryonic lethality and curbs the growth of MEFs and/or ES cells (Brown and Baltimore, 2000; Gangloff et al., 2004; Herceg et al., 2001; Murakami et al., 2004). Similarly, the lethality of Tel2 deletions in *C. elegans* and *S. cerevisiae* might be due to loss of function of essential PIKKs.

The phenotypes associated with viable mutations in the Tel2 orthologs of yeast and *C. elegans* can also be understood in the context of effects on one or more of the PIKKs. The telomere-length defect of the *S. cerevisiae tel2-1* mutant (S129N) could result from diminished activity of Tel1 and/or Mec1, which are required for telomere maintenance (Ritchie et al., 1999). The defects in the S phase checkpoint of *C. elegans clk-2/rad-5* mutants (C772Y for *clk-2* and G135C for *rad-5*) could be due to diminished expression of ATL-1, the ATR ortholog of *C. elegans*. The replication checkpoint phenotype of reduced Tel2 levels in *S. pombe* is also consistent with compromised function of its ATR ortholog (Rad3) (Shikata et al., 2007). Furthermore, the extended life span of the *clk-2* mutant could be explained by partial inhibition of LET-363, the mTOR ortholog of *C. elegans* (Vellai et al., 2003). As this aging phenotype is not observed with the *rad-5* allele, the *rad-5* G135C mutation in the *C. elegans* TEL2 ortholog might affect ATL-1 and LET-363 in different ways. Differential effects of the point mutations in TEL2 orthologs could also explain why the *S. cerevisiae tel2-1* mutant shows no overt *mec1* phenotype (e.g., sensitivity to IR, MMS, or HU [Ahmed et al., 2001]).

The mechanism by which Tel2 stabilizes the PIKKs is unknown. Tel2 could have a chaperone or cochaperone-like role, facilitating correct folding of the large PIKK polypeptides. However, several observations argue against this possibility. For instance, the localization of the PIKKs and their rate of synthesis are not strongly affected by Tel2 status, and the effect of Tel2 loss does not resemble the consequences of inhibition of the Hsp90 chaperone. It is also not known which pathway is responsible for PIKK degradation in Tel2-deficient cells. Although we anticipated that the proteasome pathway contributes to PIKK degradation, proteasome inhibitors did not stabilize the full-length PIKKs in Tel2 null cells and we did not detect ubiquitylated forms of the PIKKs. One possibility is that, rather than having a chaperone function, Tel2 protects the PIKKs from cleavage by a specific protease. The

products of this initial cleavage could then be processed by the proteasome. Such a scenario would explain why inhibition of the proteasome does not result in accumulation of the full-length PIKKs in Tel2-deficient cells.

The finding that mammalian PIKKs and possibly other eukaryotic PIKKs require Tel2 for their stability raises questions about the functional significance of this dependency. One possibility is that the universal Tel2-PIKK interaction simply reflects the divergence of the PIKKs from a common ancestor. If this primordial eukaryotic PIKK was regulated through its interaction with Tel2, this dependency may have persisted even if the original Tel2-dependent control is no longer required in the context of the newly diverged PIKKs. However, the existence of a single protein required for the stability of all PIKKs could also point to a common mechanism to govern PIKK activity that has not yet been appreciated. For instance, Tel2 could be a regulatory node that allows cells to rapidly downmodulate all PIKKs in concert. The biological utility of such a pathway is not obvious to us, especially given the diverse cellular roles of the PIKKs. Alternatively, we imagine that specific and regulated disruption of the Tel2-binding ability of individual PIKKs (e.g., by modification of the Tel2-interaction site) would allow cells to rapidly downregulate specific signaling pathways. We are currently testing a specific version of this model in which Tel2 is proposed to dissociate from each PIKK upon its activation. This mechanism would impose a shortened half-life on the activated PIKK while simultaneously allowing cells to accumulate and maintain a pool of Tel2-bound inactive forms of the same PIKK for later use. As a result, the signaling activity would be of limited duration once the original stimulus has dissipated, thus endowing cells with an intrinsic mechanism by which they can exit stress-response states. It will be interesting to determine whether these regulatory options are used by mammals and other eukaryotes and to explore the possibility that manipulation of the Tel2-PIKK interaction might be beneficial in the context of human diseases, including cancer.

EXPERIMENTAL PROCEDURES

Cell Culture

Primary MEFs were isolated from 13.5 day embryos and maintained in DMEM supplemented with 15% fetal calf serum (FCS). MEFs transformed by SV40-LT and TERT-BJ cells were cultured in medium without pyruvate with 10% FCS. HeLa S3 cells were maintained in Joklik's medium (Sigma) with 10% FBS. Media were supplemented 4-OHT (Sigma) as indicated.

Tel2 Gene Targeting

A Bac carrying the mouse *Tel2* gene was identified using the easy-to-screen high-density filters (129/Sv, Release I, Incyte Genomics) with a cDNA probe and a region containing exons 1 to 9 of Tel2 was subcloned into vector pSL301 (Invitrogen). The targeting vector, pTV-Tel2, designed to allow conditional deletion of exon 3, was constructed using the pGKneobpAlox2PGKDTA vector (a gift from T. Jacks). The resulting pTV-Tel2 was linearized with KpnI, and gene targeting of ES cells (E14 derived from 129P2/Ola) was performed using standard techniques. Correctly targeted ES were transfected with Cre recombinase (Taniguchi et al., 1998) and selected for 48 hr in 1 μg/ml puromycin to obtain clones with either the deleted *Tel2* locus ($Tel2^{DEL/+}$) or the conditional ($Tel2^{FLOX/+}$) allele. ES clones were injected into C57BL/6J blastocysts, and chimeric founders were crossed to C57BL/6J females. PCR screening of *Tel2* genomic locus was performed to identify offspring carrying the modified alleles. $Tel2^{FLOX/+}$ mice were crossed with $p53^{-/-}$ (Jacks et al., 1994) and *R26Cre-ER* transgenic mice (B6;129-*Gt(ROSA)26Sor*$^{tm1(cre/Esr1)Nat}$/J, #004847, Jackson Laboratories), (Badea et al., 2003).

Antibodies and Western Blot Analysis

Anti-mouse Tel2 antibody #1039 was affinity purified from rabbit serum immunized with a KLH-conjugated mTel2 peptide (TGLKRYLGGTED PVLPEEKEEFATC; aa 35–56). Anti-mouse Tel2 mouse polyclonal antibody was produced against GST-tagged mouse Tel2, and the serum was absorbed using bacteria extract expressing GST-tag. Rabbit antibody TelC was raised against human Tel2 produced in insect cells and affinity purified. Rabbit anti-human Tel2 antibody #B was affinity purified from rabbit serum immunized with KLH-conjugated hTel2 peptide (RSKTQRLSKGGPRQGPAGSPSRFC; aa 670–692). Other antibodies are rabbit anti-mouse Rif1 antibody #1240 (a gift from S. Buonomo), ATM MAT3 (a gift from M. Kastan), ATR N-19 (sc-1887, Santa Cruz Biotechnology), DNA-PKcs Ab-4 (MS-423, Lab Vision), mTOR (#2972, Cell Signaling Technology), SMG1 (A300-393A, Bethyl Laboratories), TRRAP (RPH800, Serotec), AKT pS473 (#9271, Cell Signaling Technology), ATRIP (MAB1579, R&D Systems), Chk1 (sc-8408, Santa Cruz Biotechnology), Chk1 pS345 (#2348, Cell Signaling Technology), Chk2 (611570, BD Biosciences), γ-tubulin GTU-88 (T6557, Sigma), MCM2 (559542, BD PharMingen), PARP1 (NB100-112, Novus), PI3-kinase p110γ (#4254, Cell Signaling Technology), p16 M-156 (sc-1207, Santa Cruz Biotechnology), p21 F-5 (sc-6246, Santa Cruz Biotechnology), p27 (sc-528, Santa Cruz Biotechnology), p53 Al25-13 (a gift from K. Helin [Pasini et al., 2004]), p53 phospho-Serine 15 (#9284, Cell Signaling Technology), p70-S6K pT389 (#9234, Cell Signaling Technology), 53BP1 (a gift from T. Halazonetis), and TRF1 (371).

For whole cell lysates, 2×10^6 cells/10 cm dish plated 24 hr prior to harvesting were rinsed with cold PBS, and 500 μl of 2× Laemmli buffer was added. Protein samples were separated by SDS-PAGE and blotted to either nitrocellulose or PVDF (for ATM) membranes. The blots were blocked in 5% nonfat powdered milk in PBS-T (0.1% Tween-20 in PBS) for 30 min and incubated with primary antibodies in 0.1% or 1% milk in PBS-T at room temperature for at least for 1 hr. For phosphospecific antibodies, blots were treated according to the manufacturers protocol.

FACS Analysis

MEFs were pulse labeled with 10 μM BrdU (Sigma) for 60 min, harvested by trypsinization, fixed in 70% ethanol, and stored at −20°C. Fixed cells were incubated with FITC-conjugated anti-BrdU antibodies (BD PharMingen) according to the manufactur's protocol and counterstained with a propidium iodide buffer containing 100 μg/ml RNase, 5 μg/ml propidium iodide (Sigma), and 0.5% (W/V) BSA in PBS. Flow cytometry was performed with a FACScalibur (Becton Dickinson). Data were analyzed with either CELL Quest software (Becton Dickinson) or FlowJo (Tree Star).

Tel2 Knockdown by shRNA

Phoenix cells were used to produce shRNA expressing pSUPER.retro (OligoEngine) retroviruses. Recipient BJ-hTERT cells were infected four times every 12 hr and selected in puromycin. Target sequences were as follows: luciferase, 5′-CGT ACG CGG AAT ACT TCG A-3′; hTel2-sh2, 5′-GGA ACC TGG TGG TGA AGA A-3′; hTel2-sh5, 5′-GGA GAG TGC AGA TGC AGG A-3′; hTel2-sh6, 5′-AGA AGC TTC TGT TCT TAC A-3′. Inducible expression of Tel2 shRNA in mouse ES cells was as described by Seibler and colleagues (Seibler et al., 2007).

Proteomic Analysis and Immunoprecipitations

Isolation of the human Tel2 complex was performed by FLAG-HA tandem affinity purification as described previously (Ye and de Lange, 2004). Eluted proteins were separated by SDS-PAGE (8%–16% gradient, Invitrogen) and the protein bands were excised and subjected to trypsin digestion. The resulting peptides were extracted, and the proteins were identified by mass spectrometry at the Rockefeller University Proteomics Resource Center.

Tel2 immunoprecipitations from MEFs were performed using one 15 cm plate of MEFs expressing myc-tagged human full-length Tel2. The cells were rinsed in cold PBS, scraped in 1 ml lysis buffer (50 mM Tris-HCl pH 7.6, 150 mM NaCl, 1 mM EDTA, 1 mM PMSF, 1 μg/ml Aprotinin, 2 μg/ml Pepstatin, 1 μg/ml Leupeptin [Roche]), and disrupted by sonication. Lysate was centrifuged at 16,000 g for 15 min at 4°C. The supernatant was used as the input lysate. Fifty μl of anti-myc Agarose bead (A7470, Sigma) slurry (50% [v/v] in PBS, blocked with 10% BSA in PBS) was added to 0.5–1 ml of lysate. Samples were nutated at 4°C for at least 2 hr. The beads were washed four times with lysis buffer. After removal of buffer, the beads were suspended in 50 μl 2× Laemmli buffer.

Interaction of endogenous Tel2 and PIKKs were analyzed as below. 1×10^8 HeLa S3 cells were collected, rinsed in cold PBS, and disrupted by homogenization in 1 ml of lysis buffer (10 mM Tris-HCl pH 7.6, 150 mM KCl, 1.5 mM $MgCl_2$, 5 mM β-mercaptoethanol,1 mM PMSF, and 1× complete protease inhibitor [Roche]) on ice. The lysate was cleared by centrifugation at 16,000 g for 15 min at 4°C, incubated with protein G-Sepharose beads (GE Healthcare), centrifuded again. The supernatant was used for the immunoprecipitation with Tel2C, preimmune serum, or TRF1 antibody. The beads were washed four times with lysis buffer. After removal of buffer, the beads were suspended in 80 μl 2× Laemmli buffer.

Northern Blot Analysis and RT-PCR Analysis

Total cellular RNA was prepared using Trizol reagent (GIBCO) according to the manufactur's protocol, and northern blot analysis was performed as described previously (Watanabe et al., 1995). Northern probes were prepared by RT-PCR as described in the Supplemental Data. The cDNA probes amplified by PCR were labeled with [^{32}P]dCTP by random priming. GAPDH mRNA served as an internal control.

Metabolic Labeling and Immunoprecipitation

One day prior to labeling 1.5×10^6 cells were plated per 10 cm dish. Cells were rinsed with methionine and cysteine (met/cys) free DMEM (#21013-024, GIBCO) three times and incubated with 4 ml labeling medium (met/cys-free DMEM, 10% dialyzed FBS, 2 mM L-glutamine) containing 0.1 mCi/ml of a [^{35}S]-met/cys mix (Expre^{35}S ^{35}S protein labeling mix, #NEG772007MC, NEN) for 1 hr. The medium was replaced with normal culture medium (15% FCS, 0.1 mM nonessential amino acids, 100 units/ml of penicillin, 0.1 mg/ml streptomycin, and 2 mM L-glutamine in DMEM) supplemented with 15 μg/ml L-metionine and L-cysteine-HCl (Sigma). IPs were performed as described (Ye and de Lange, 2004) with ATM Ab MAT2 (a gift from Y. Shiloh) and mTOR Ab #2972 (Cell Signaling Technology). Precipitates were lysed in 2× Laemmli buffer and separated by SDS-PAGE. The gels were immersed in Amplify (NAMP100V, Amersham) and dried and exposed to a PhosphoImager screen (GE Healthcare). The quantification of the signal incorporated into ATM and mTOR proteins was done with the Storm imaging system and the ImageQuant software (GE Healthcare).

In Vitro Binding Assays

ATM and mTOR cDNA fragments were amplified by PCR using human ATM and rat mTOR cDNAs, respectively, and cloned into pGEX-4T-2. GEX-4T-2 transformed BL21 cells were grown up in 1 l of 2xYT medium, and 0.2 mM IPTG was added when the OD_{600} was ~0.5. After 3 hr at 30°C, cells were harvested, resuspended in 16 ml of lysis buffer (50 mM Tris [pH 8.0], 100 mM KCl, 1% Triton X-100, 2 mM DTT, 1 μg/ml lysozyme, 0.1 mM PMSF, and 1× Complete protease inhibitor mix [Roche]) and sonicated on ice. The lysate was cleared by centrifugation at 40,000 g for 20 min at 4°C and incubated with 500 μl of equilibrated glutathione beads for 2 hr at 4°C. Beads were washed three times in PBS containing 2 mM DTT, 0.1 mM PMSF, 1× Complete protease inhibitor, and once in wash buffer 2 (50 mM Tris [pH 8.0], 100 mM KCl, 10% glycerol, 2 mM DTT, 0.1 mM PMSF). Fusion proteins were eluted in 500 μl of wash buffer 2 containing 20 mM glutathione (reduced form). Three sequential elutions were collected and dialyzed against PBS/10% glycerol. Five micrograms of GST-fusion protein or GST alone were incubated with 2 μg of baculovirally expressed Tel2 or TRF1 in binding buffer (20 mM Tris [pH 8.0], 100 mM KCl, 1.5 mM $MgCl_2$, 10% glycerol, 5 mM β-mercaptoethanol, 1 mg/ml BSA, 1× Complete [-EDTA] protease inhibitor) at 4°C for 1 hr. Glutathione beads (20 μl) were added and incubated for 1 hr at 4°C. Beads were collected at 500 g, washed three times with binding buffer, and bound protein was eluted in Laemmli buffer.

Supplemental Data

Supplemental Data include six figures, Supplemental Experimental Procedures, and Supplemental References and can be found with this article online at http://www.cell.com/cgi/content/full/131/7/1248/DC1/.

ACKNOWLEDGMENTS

We gratefully acknowledge Jost Seibler and Holger Kissel (Artemice Pharmaceuticals GmbH) for the inducible Tel2 knockdown in ES cells. Devon White is thanked for outstanding mouse husbandry and the RU Gene Targeting and Transgenic Facilities and Chinweng Yang for help in generating gene targeted mice. We thank Tyler Jacks, Mike Kastan, Yosef Shiloh, John Petrini, Noboru Motoyama, Noriko Oshiro, and Kristian Helin for reagents and materials. Jill Donigian, Eros Lazzerini Denchi, Dirk Hockemeyer, Sara B.C. Buonomo, and other member of the de Lange laboratory are thanked for discussion and comments on this manuscript. R.C.W. was supported by an NIH MSTP grant (GM07739) to the Cornell/RU/MSK Tri-Institutional MD/PhD program. This research was supported by grants from the Breast Cancer Research Foundation and the NCI (CA076027) to T.d.L. H.T. and T.d.L. planned the experiments and wrote the paper together. H.T. made the figures and executed all experiments except for those in Figure S1 (performed by RCW), Figure S8 (performed by HY), and Figures 6E and 6F (performed by K.K.T.).

Received: April 23, 2007
Revised: July 27, 2007
Accepted: October 30, 2007
Published: December 27, 2007

REFERENCES

Abraham, R.T. (2001). Cell cycle checkpoint signaling through the ATM and ATR kinases. Genes Dev. *15*, 2177–2196.

Ahmed, S., Alpi, A., Hengartner, M.O., and Gartner, A. (2001). C. elegans RAD-5/CLK-2 defines a new DNA damage checkpoint protein. Curr. Biol. *11*, 1934–1944.

Andrade, M.A., and Bork, P. (1995). HEAT repeats in the Huntington's disease protein. Nat. Genet. *11*, 115–116.

Badea, T.C., Wang, Y., and Nathans, J. (2003). A noninvasive genetic/pharmacologic strategy for visualizing cell morphology and clonal relationships in the mouse. J. Neurosci. *23*, 2314–2322.

Bakkenist, C.J., and Kastan, M.B. (2004). Initiating cellular stress responses. Cell *118*, 9–17.

Benard, C., McCright, B., Zhang, Y., Felkai, S., Lakowski, B., and Hekimi, S. (2001). The C. elegans maternal-effect gene clk-2 is essential for embryonic development, encodes a protein homologous to

yeast Tel2p and affects telomere length. Development *128*, 4045–4055.

Bosotti, R., Isacchi, A., and Sonnhammer, E.L. (2000). FAT: a novel domain in PIK-related kinases. Trends Biochem. Sci. *25*, 225–227.

Brown, E.J., and Baltimore, D. (2000). ATR disruption leads to chromosomal fragmentation and early embryonic lethality. Genes Dev. *14*, 397–402.

Celli, G., and de Lange, T. (2005). DNA processing not required for ATM-mediated telomere damage response after TRF2 deletion. Nat. Cell Biol. *7*, 712–718.

Collis, S.J., Barber, L.J., Clark, A.J., Martin, J.S., Ward, J.D., and Boulton, S.J. (2007). HCLK2 is essential for the mammalian S-phase checkpoint and impacts on Chk1 stability. Nat. Cell Biol. *9*, 391–401.

Conti, E., and Izaurralde, E. (2005). Nonsense-mediated mRNA decay: molecular insights and mechanistic variations across species. Curr. Opin. Cell Biol. *17*, 316–325.

Feil, R., Brocard, J., Mascrez, B., LeMeur, M., Metzger, D., and Chambon, P. (1996). Ligand-activated site-specific recombination in mice. Proc. Natl. Acad. Sci. USA *93*, 10887–10890.

Gangloff, Y.G., Mueller, M., Dann, S.G., Svoboda, P., Sticker, M., Spetz, J.F., Um, S.H., Brown, E.J., Cereghini, S., Thomas, G., and Kozma, S.C. (2004). Disruption of the mouse mTOR gene leads to early postimplantation lethality and prohibits embryonic stem cell development. Mol. Cell. Biol. *24*, 9508–9516.

Greenwell, P.W., Kronmal, S.L., Porter, S.E., Gassenhuber, J., Obermaier, B., and Petes, T.D. (1995). TEL1, a gene involved in controlling telomere length in S. cerevisiae, is homologous to the human ataxia telangiectasia gene. Cell *82*, 823–829.

Guertin, D.A., and Sabatini, D.M. (2005). An expanding role for mTOR in cancer. Trends Mol. Med. *11*, 353–361.

Hartman, P.S., and Herman, R.K. (1982). Radiation-sensitive mutants of Caenorhabditis elegans. Genetics *102*, 159–178.

Hay, N., and Sonenberg, N. (2004). Upstream and downstream of mTOR. Genes Dev. *18*, 1926–1945.

Herceg, Z., Hulla, W., Gell, D., Cuenin, C., Lleonart, M., Jackson, S., and Wang, Z.Q. (2001). Disruption of Trrap causes early embryonic lethality and defects in cell cycle progression. Nat. Genet. *29*, 206–211.

Herceg, Z., and Wang, Z.Q. (2005). Rendez-vous at mitosis: TRRAPed in the chromatin. Cell Cycle *4*, 383–387.

Jacks, T., Remington, L., Williams, B.O., Schmitt, E.M., Halachmi, S., Bronson, R.T., and Weinberg, R.A. (1994). Tumor spectrum analysis in p53-mutant mice. Curr. Biol. *4*, 1–7.

Jiang, N., Benard, C.Y., Kebir, H., Shoubridge, E.A., and Hekimi, S. (2003). Human CLK2 links cell cycle progression, apoptosis, and telomere length regulation. J. Biol. Chem. *278*, 21678–21684.

Kastan, M.B., and Bartek, J. (2004). Cell-cycle checkpoints and cancer. Nature *432*, 316–323.

Lakowski, B., and Hekimi, S. (1996). Determination of life-span in Caenorhabditis elegans by four clock genes. Science *272*, 1010–1013.

Lavin, M.F., Khanna, K.K., Beamish, H., Spring, K., Watters, D., and Shiloh, Y. (1995). Relationship of the ataxia-telangiectasia protein ATM to phosphoinositide 3-kinase. Trends Biochem. Sci. *20*, 382–383.

Lustig, A.J., and Petes, T.D. (1986). Identification of yeast mutants with altered telomere structure. Proc. Natl. Acad. Sci. USA *83*, 1398–1402.

Morrow, D.M., Tagle, D.A., Shiloh, Y., Collins, F.S., and Hieter, P. (1995). TEL1, an S. cerevisiae homolog of the human gene mutated in ataxia telangiectasia, is functionally related to the yeast checkpoint gene MEC1. Cell *82*, 831–840.

Murakami, M., Ichisaka, T., Maeda, M., Oshiro, N., Hara, K., Edenhofer, F., Kiyama, H., Yonezawa, K., and Yamanaka, S. (2004). mTOR is essential for growth and proliferation in early mouse embryos and embryonic stem cells. Mol. Cell. Biol. *24*, 6710–6718.

Pasini, D., Bracken, A.P., Jensen, M.R., Lazzerini Denchi, E., and Helin, K. (2004). Suz12 is essential for mouse development and for EZH2 histone methyltransferase activity. EMBO J. *23*, 4061–4071.

Perry, J., and Kleckner, N. (2003). The ATRs, ATMs, and TORs are giant HEAT repeat proteins. Cell *112*, 151–155.

Pimpinelli, S. (2005). *Drosophila* Telomeres. In Telomeres, T. de Lange, V. Lundblad, and E. Blackburn, eds. (Cold Spring Harbor, New York: Cold Spring Harbor Laboratory Press), pp. 433–464.

Ritchie, K.B., Mallory, J.C., and Petes, T.D. (1999). Interactions of TLC1 (which encodes the RNA subunit of telomerase), TEL1, and MEC1 in regulating telomere length in the yeast Saccharomyces cerevisiae. Mol. Cell. Biol. *19*, 6065–6075.

Runge, K.W., and Zakian, V.A. (1996). TEL2, an essential gene required for telomere length regulation and telomere position effect in Saccharomyces cerevisiae. Mol. Cell. Biol. *16*, 3094–3105.

Sabatini, D.M. (2006). mTOR and cancer: insights into a complex relationship. Nat. Rev. Cancer *6*, 729–734.

Seibler, J., Kleinridders, A., Kuter-Luks, B., Niehaves, S., Bruning, J.C., and Schwenk, F. (2007). Reversible gene knockdown in mice using a tight, inducible shRNA expression system (. Nucleic Acids Res. *35*, e54.

Shaw, R.J., and Cantley, L.C. (2006). Ras, PI(3)K and mTOR signalling controls tumour cell growth. Nature *441*, 424–430.

Shikata, M., Ishikawa, F., and Kanoh, J. (2007). Tel2 is required for activation of the mrc1-mediated replication checkpoint. J. Biol. Chem. *282*, 5346–5355.

Shiloh, Y. (2003). ATM and related protein kinases: safeguarding genome integrity. Nat. Rev. Cancer *3*, 155–168.

Silver, D.P., and Livingston, D.M. (2001). Self-excising retroviral vectors encoding the Cre recombinase overcome Cre-mediated cellular toxicity. Mol. Cell *8*, 233–243.

Silverman, J., Takai, H., Buonomo, S.B., Eisenhaber, F., and de Lange, T. (2004). Human Rif1, ortholog of a yeast telomeric protein, is regulated by ATM and 53BP1 and functions in the S-phase checkpoint. Genes Dev. *18*, 2108–2119.

Takai, H., Smogorzewska, A., and de Lange, T. (2003). DNA damage foci at dysfunctional telomeres. Curr. Biol. *13*, 1549–1556.

Taniguchi, M., Sanbo, M., Watanabe, S., Naruse, I., Mishina, M., and Yagi, T. (1998). Efficient production of Cre-mediated site-directed recombinants through the utilization of the puromycin resistance gene, pac: a transient gene-integration marker for ES cells. Nucleic Acids Res. *26*, 679–680.

Vellai, T., Takacs-Vellai, K., Zhang, Y., Kovacs, A.L., Orosz, L., and Muller, F. (2003). Genetics: influence of TOR kinase on lifespan in C. elegans. Nature *426*, 620.

Watanabe, K., Yamada, H., and Yamaguchi, Y. (1995). K-glypican: a novel GPI-anchored heparan sulfate proteoglycan that is highly expressed in developing brain and kidney. J. Cell Biol. *130*, 1207–1218.

Wullschleger, S., Loewith, R., and Hall, M.N. (2006). TOR signaling in growth and metabolism. Cell *124*, 471–484.

Xu, L., and Blackburn, E.H. (2004). Human Rif1 protein binds aberrant telomeres and aligns along anaphase midzone microtubules. J. Cell Biol. *167*, 819–830.

Ye, J.Z., and de Lange, T. (2004). TIN2 is a tankyrase 1 PARP modulator in the TRF1 telomere length control complex. Nat. Genet. *36*, 618–623.

Cell, Volume *131*

Supplemental Data

Tel2 Regulates the Stability of PI3K-Related Protein Kinases

Hiroyuki Takai, Richard C. Wang, Kaori K. Takai, Haijuan Yang, and Titia de Lange

Supplemental Experimental Procedures

Cell culture

Primary mouse embryonic fibroblasts (MEFs) were isolated from 13.5 day embryos and maintained in DMEM supplemented with 15% (V/V) fetal calf serum (FCS), 0.1 mM non-essential amino acids, 100 units/ml of penicillin, 0.1 mg/ml streptomycin, 1 mM Sodium pyruvate, and 2 mM L-glutamine (Gibco). MEFs harboring the wild type or heterozygus *Tel2* allele isolated from the same litter were used as control cells. MEFs transformed by SV40-LT and TERT-BJ cells were cultured in medium without pyruvate and with 10% FCS. HeLa S3 cells were maintained in Joklik's medium (Sigma) supplemented with 10% of Fetal Bovine Serum and 0.1 mM nonessential amino acids, 100 units/ml of penicillin, 0.1 mg/ml streptomycin and 2 mM L-glutamine (Gibco). Media were supplemented with 4-Hydroxytamoxifen (4-OHT) (Sigma), wortmannin (Sigma), or rapamycin (Calbiochem) as indicated.

Tel2 gene targeting

The mouse *Tel2* gene was isolated by screening an Easy-to-screen™ High-Density Filters: Bac Mouse (129/Sv, Release I, Incyte Genomics) with mouse Tel2 cDNA as a probe. A 16 kb fragment of genomic DNA containing exon 1 to 9 of Tel2 was subcloned into the pSL301 vector (Invitrogen). The targeting vector, pTV-Tel2 was constructed using the pGKneobpAlox2PGKDTA vector (, which includes a PGK-Neo cassette flanked by the *lox*P site and a negative selection DTA cassette. The targeting vector was designed to enable conditional deletion of exon 3. The *Sca*I-*Kpn*1 fragment containing exons 1-3 was modified by inserting a *lox*P site and an *Nde*I site into the ApaI site. This fragment was inserted in between the DTA cassette and the neo marker of the pGKneobpAlox2PGKDTA vector. On the other end of the neo cassette, a 5.2-kb *Kpn*I containing exons 4 to 8 was inserted downstream of the *lox*P site. The vector was linearized with *Kpn*I, and gene targeting was performed following standard

techniques using the embryonic stem (ES) cell line E14 derived from 129P2/Ola. ES cell clones containing the correct integration event were identified by genomic blotting of *Nde*I-digested genomic DNA using probes p1 and p2 shown in Figure 1A. Cre recombinase was introduced transiently by electroporation of the pCre-pac plasmid (Taniguchi et al., 1998) into appropriately targeted ES cell clones and selected for 48 h in 1 μg/ml puromycin to obtain clones with either the deleted *Tel2* locus ($Tel2^{DEL/+}$) or the conditional ($Tel2^{FLOX/+}$) allele. ES cell clones were again screened by genomic blotting. Targeted ES cell clones were injected into C57BL/6J blastocysts, and chimeric founders were crossed to C57BL/6J females. All mice were maintained in a specific pathogen-free animal facility at The Rockefeller University. Polymerase chain reaction (PCR) screening of *Tel2* genomic locus was performed using the following primers: f1, 5'-TCC ACT TCT CAG CCG TCC TTA GAT-3'; r1, 5'-ACA AGG ATC CAT AGC AGC AAT GTG-3'; and r2, 5'-CTT CCC AAG AAC TCG AGA TAC GAA-3'. Primers f1 and r1 amplify the wild-type (WT, 645 bp) and 'floxed' (flanked by *lox*P sites, FLOX) alleles (687 bp); f1 and r2 primers amplify the deletion allele (DEL, 1.2 kb). PCRs were performed at 94 °C for 5 min and 30 cycles of 94 °C for 30 s, 62 °C for 30 s, 72 °C for 30s. $Tel2^{FLOX/+}$ mice were crossed with $p53^{-/-}$ (Jacks et al., 1994) and *R26Cre-ER* transgenic mice (B6;129-$Gt(ROSA)26Sor^{tm1(cre/Esr1)Nat}$/J, #004847, Jackson Laboratories), (Badea et al., 2003).

Antibodies

Anti-human Tel2 antibody #A was affinity purified from rabbit serum immunized with KLH-conjugated hTel2 peptide (RSKTQRLSKGGPRQGPAGSPSRFC representing amino acids 670-692 plus a Cys residue). Additional antibodies used for Western blot, immunofluorescence and ChIP analysis were as follows; AKT (#9272, Cell Signaling Technology); BRCA1 (Ab-1) (OP92, Oncogene); Histone H3 phospho-Serine 10 (#9706, Cell Signaling); Smc1 (A300-055A, Bethyl Laboratories); FLAG (M2) (F-3165, Sigma); Rent1 (A300-038A, Bethyl Laboratories); NBS1 (93-6', a gift from J. Petrini); PTEN (ABM-2052, Cascade); PCNA (#555566, BD Pharmingen); Raptor (W990) (#2214, Cell Signaling Technology).

Inducible depletion of *Tel2* gene in ES cells

$Tel2^{FLOX/TARGET}$ and $Tel2^{FLOX/NEO}$ ES cells were established by retargeting the $Tel2^{FLOX/+}$ ES cells with the linearized pTV-Tel2 vector. ES cell clones were screened by genomic blotting. Appropriately targeted ES cell clones were transfected with pCXH-CreER and

selected against hygromycin B. ES cell clones were again screened by genomic blotting and tested for their OHT-inducible Cre mediated recombination of the Tel2 locus.

Plasmids and retroviral gene delivery

Tagged alleles of Tel2 were cloned by PCR from a full-length cDNA clone (RZPD ID: DKFZp434A073) into the pLPC vector. Retroviral gene delivery was performed as described (Karlseder et al., 2002) except that cells were infected 3 times at 12 hr intervals. Briefly, phoenix packaging cells (293T derived cell lines) were transfected with 15 μg of the relevant plasmid DNA. The media was refreshed 12 hrs later. 36 hours after the transfection, the media, containing viral particles, was filtered through a 0.5 μm filter and combined with 4 μg/ml polybrene. This mixture was placed on target cells and repeated twice at 12 hr intervals.

Immunofluorescence and Chromatin Immunoprecipitation (ChIP)

Cells grown on coverslips were fixed with 2% paraformaldehyde in PBS for 10 min at room temperature, washed with PBS, permeabilized with 0.5% NP-40 in PBS for 10 min at room temperature and washed three times with PBS. Cells were blocked with PBG containing 0.2% (v/v) cold water fish gelatin (Sigma), 0.5% (w/v) BSA in PBS for at least 30 minutes and incubated for 2 hr at room temperature with indicated antibodies in PBG. Anti-mouse and rabbit immunoglobulin conjugated with Alexa 488 (Molecular Probes) and Rhodamine Red-X (RRX, Jackson) were used as secondary antibodies. ChIP was performed as previously described (Loayza and de Lange, 2003).

Northern blot analysis and RT-PCR analysis

Total cellular RNA was prepared using Trizol reagent (Gibco) according to the manufactur's protocol, and Northern blot analysis was performed as described previously (Watanabe et al., 1995). Northern probes were prepared by RT-PCR. The first strand cDNA was synthesized using total RNA from E14 mouse ES cells with ThermoScript RT-PCR System (Invitrogen) and amplified by PCR with oligonucleotide primers as follows: mouse *ATM* cDNA was amplified by PCR with sense #1 (5'- AAC ACT GCG AAG ATA AAG AAG AGC -3') and antisense #1 (5'- AGA TCG GCC TAA GAA CCT GAG C -3'), sense #2 (5'- GCA AGC CGC TCA GCA ACT CCT -3') and antisense #2 (5'- CTC AGC GCA CCA CTC TCG TCT TT -3'), mouse TOR cDNA was amplified by PCR with sense #1 (5'- CAT GCC GCT GTC CTC GTT CTC -3') and

antisense #1 (5'- GCG GGG CAG CAG GTT AAG GAT TGT -3'), sense #2 (5'- CAG CGG GGC CAA CAT CAC CAA T -3') and antisense #2 (5'- ACA TGC CTT TCA CGT TCC TCT CC -3'), mouse ATR cDNA was amplified by PCR with sense #1 (5'- AAG CCG AGC CAT CCC TGA A -3') and antisense #1 (5'- AAT CCG GCC TTT TGT TGA GAC TTA -3'), sense #2 (5'- TCT TAT CCC ATG CGT GTG AAC -3') and antisense #2 (5'- CCA AGC CCC AGG ATG TAG C -3'), mDNA-PKcs cDNA was amplified by PCR with sense #1 (5'- ATC CCA TCG ATC ACC TAA GAC G -3') and antisense #1 (5'- CAT CGC CAA TAT TGA AAC CTA AGC -3'), sense #2 (5'- CTG AAC CACTGC CGG AGC CAC AC -3') and antisense #2 (5'- GAA CTG CCA GCA AGG AAT AGA TGA -3'), mouse GAPDH cDNA was amplified by PCR with sense #1(5'- GGG TGA GGC CGG TGC TGA GTA T -3') and antisense #2 (5'- TTG GGG GTA GGA ACA CGG AAG G -3'). PCR products were subcloned into pCR-script Amp (Stratagene). Northern probes for *SMG1* and *TRRAP* were amplified by PCR using IMAGE clones 4972483 and 33014889, respectively as templates with oligonucleotide primers as follows: mouse *SMG1* cDNA was amplified by PCR with sense #1 (5'- GCC TGG ATG CTG CCT TAT TT -3') and antisense #1 (5'- TGT TGT CTT GCC ATG ATT TGT ATT -3'), sense #2 (5'- TTG CTG CAG CGG TTA GGA GTA -3') and antisense #2 (5'- TGA GGC TGA GTT GAT TCT GGT G -3'), mouse *TRRAP* cDNA was amplified by PCR with sense #1 (5'- GCC TTC ACT GGT CGT TTC CTG T -3') and antisense #1 (5'- GTT GCG GTT CTT GTT GTT GTC A -3'), sense #2 (5'- TGC TCC CGT CCA TTA CCA AC -3') and antisense #2 (5'- TCT CGC TGA ACC TGA TGA CTG C -3'). The cDNA probes were amplified by PCR and labeled with [^{32}P]dCTP by the random priming. GAPDH mRNA served as an internal control.

RT-PCR detection of ATM mRNA

For semi-quantitative RT-PCR, total RNA from MEFs was isolated by using Trizol reagent (Gibco) according to the manufactur's protocol. 1.25 μg of total RNA was subjected to reverse transcription using random oligo primer and ThermoScript RT-PCR System (Invitrogen) according to the manufactur's protocol. PCR was performed using the primer pairs, ATM sense #1 and antisense #1, as described above. PCR cycles were setup as follows: for ATM and *Gapdh*, denaturing for 30 sec at 94 °C, annealing for 40 sec at 58 °C and elongation for 30 sec at 72 °C. PCR products were examined every 4 cycles to confirm the linearity of the PCR. The primer set used here gave single bands with expected sizes. Amplified cDNAs were confirmed by DNA sequencing.

SUPPLEMENTAL REFERENCES

Badea, T. C., Wang, Y., and Nathans, J. (2003). A noninvasive genetic/pharmacologic strategy for visualizing cell morphology and clonal relationships in the mouse. J Neurosci *23*, 2314-2322.

Jacks, T., Remington, L., Williams, B. O., Schmitt, E. M., Halachmi, S., Bronson, R. T., and Weinberg, R. A. (1994). Tumor spectrum analysis in p53-mutant mice. Curr Biol *4*, 1-7.

Karlseder, J., Smogorzewska, A., and de Lange, T. (2002). Senescence induced by altered telomere state, not telomere loss. Science *295*, 2446-2449.

Loayza, D., and de Lange, T. (2003). POT1 as a terminal transducer of TRF1 telomere length control. Nature *424*, 1013-1018.

Taniguchi, M., Sanbo, M., Watanabe, S., Naruse, I., Mishina, M., and Yagi, T. (1998). Efficient production of Cre-mediated site-directed recombinants through the utilization of the puromycin resistance gene, pac: a transient gene-integration marker for ES cells. Nucleic Acids Res *26*, 679-680.

Watanabe, K., Yamada, H., and Yamaguchi, Y. (1995). K-glypican: a novel GPI-anchored heparan sulfate proteoglycan that is highly expressed in developing brain and kidney. J Cell Biol *130*, 1207-1218.

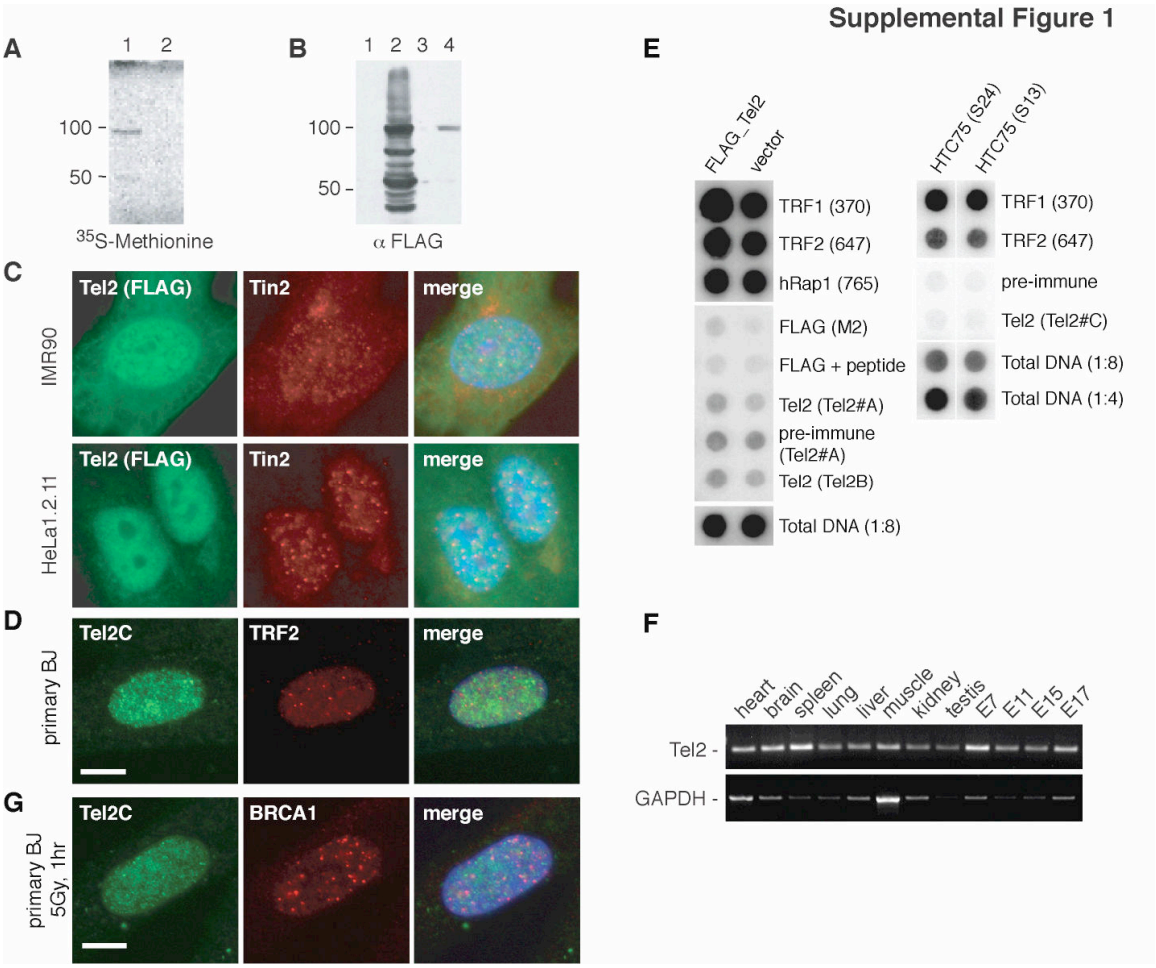

Figure S1. hTel2 does not associate with telomeres.

(A) Verification of the Tel2 expression construct. The human Tel2 cDNA (RZPD DKFZp434A073) (lane 1) and a truncated cDNA lacking the predicted start codon were used for in vitro translation (IVT). IVT products were detected based on incorporation of ^{35}S-methionine. MWs are indicated in kDa.

(B) Expression of tagged human Tel2 in vivo. Immunoblots of 293T cells transiently transfected with vector control (lane 1) or FLAG-Tel2 (lane 2), and IMR90 fibroblasts infected with the retroviral vector control (lane 3) or FLAG-Tel2 (lane 4). FLAG-Tel2 was detected with anti-Flag (M2) antibody.

(C) Localization of FLAG-Tel2 in retrovirally infected IMR90 fibroblasts and HeLa cells. Cells were stained with FLAG (M2, green) and TIN2 (865; red) as a marker for telomeres. FLAG-Tel2 shows weak cytoplasmic and strong, diffuse nuclear staining in methanol fixed IMR90 and HeLa1.2.11 cells.

(D) Localization of endogenous Tel2 by IF. Primary BJ fibroblasts were fixed and co-stained for Tel2 (Tel2C; green) and TRF2 (Upstate anti-TRF2; red). Images are merged with DAPI (blue) on right. Scale bar: 10 μm.

(E) No detectable association of human Tel2 with telomeric DNA. Telomeric ChIP on HeLa1.2.11 cells infected with vector or FLAG-Tel2 or two clones of HTC75 cells that do not express exogenous Tel2 using the indicated antibodies or pre-immune serum (PI). Dot blots were hybridized with a TTAGGG repeat probe and quantified. Tel2 brought down <1% of the telomeric DNA which is in the same range as background signals obtained with PI.

(F) Mouse *Tel2* mRNA is ubiquitously expressed. A MTC Multiple Tissue cDNA Panel (Mouse I, Clontech) was analyzed by PCR for Tel2 expression.

(G) Tel2 does not localize to sites of DNA damage. IF analysis of Tel2 and BRCA1 in primary BJ fibroblasts treated with IR and analyzed after 1 hr.

Supplemental Figure 2

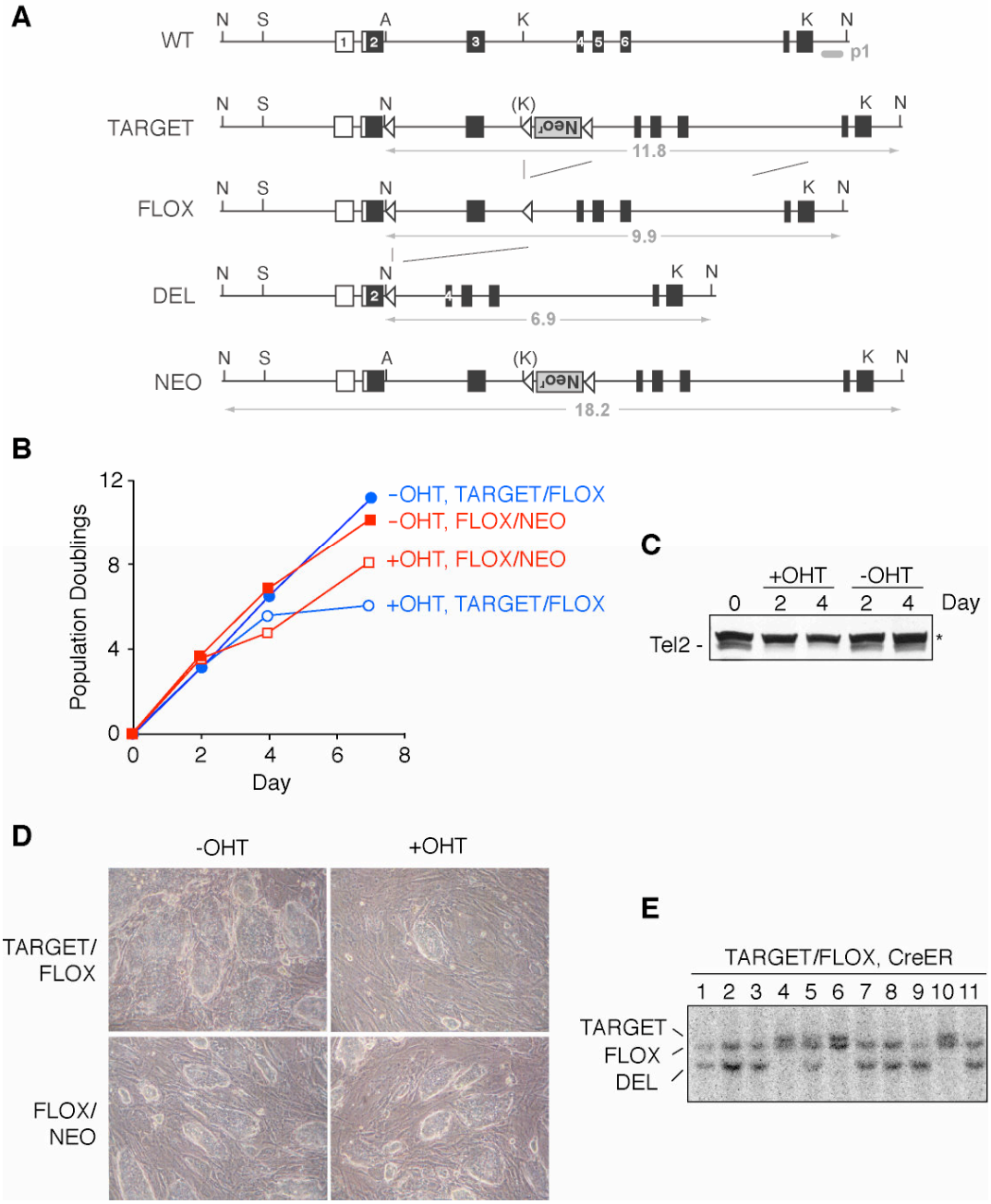

Figure S2. Tel2 is required for growth of ES cells.

(A) Schematic drawing of the mutated mouse Tel2 locus. *Nde*I fragment sizes are indicated for each genotype and the probe p1 is shown. N; *Nde*I, S; *Sca*I, K; *Kpn*I, A; *Apa*I.

(B) Growth curves of ES cells with indicated genotype treated with or without OHT to induce Cre.

(C) Tel2 immunoblots on extracts from the cells used in B. *, non-specific signals detected by the antibody.

(D) Phase-contrast microscopy images of the ES cells with indicated genotype taken at day 7 of OHT treatment. ES cells were cultured on feeder cells.

(E) Lack of recovery of Tel2 deficient ES cell lines. Conditional Tel2 ES cells were treated with Cre (low level of induction) and clones were isolated. Shown is the genotyping of the clones using genomic blots of *Nde*I digested DNA probed with probe p1 (see A).

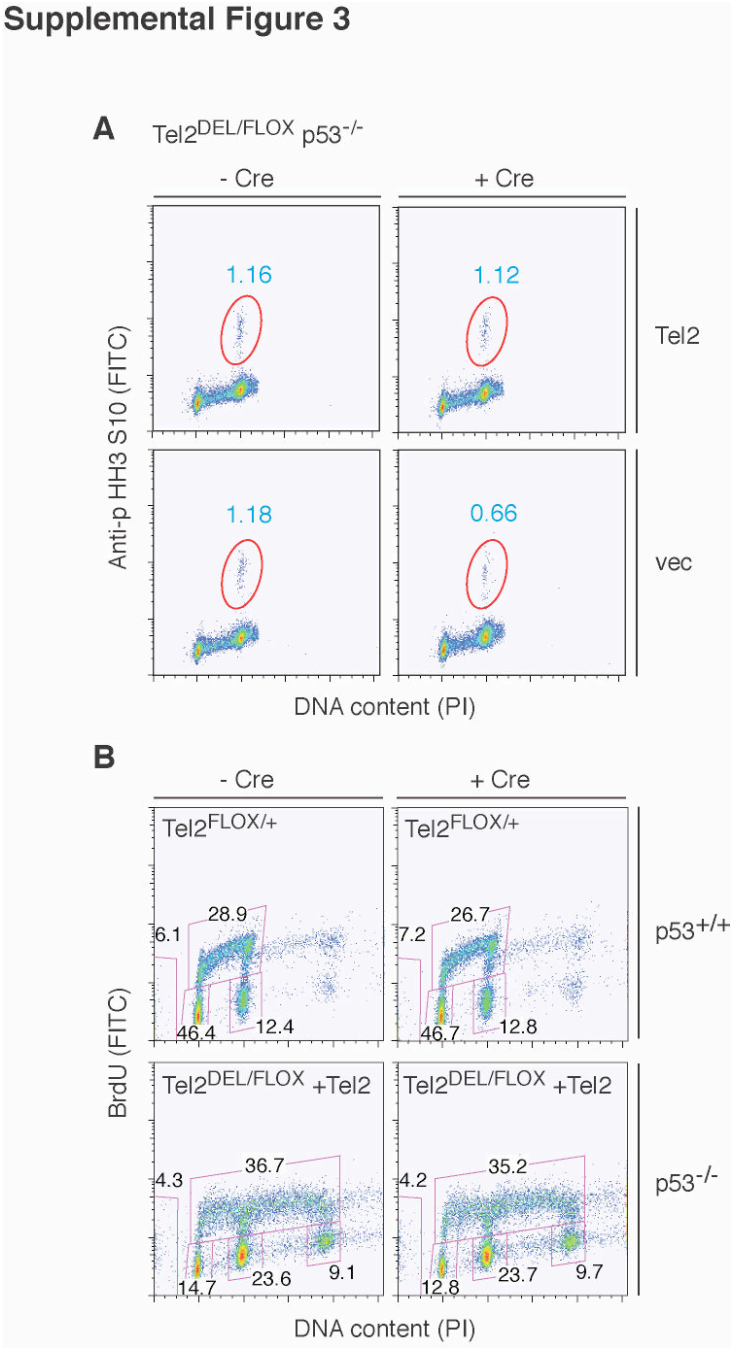

Figure S3. Tel2 deletion results in cell cycle arrest in *p53*$^{-/-}$ MEFs.

(A) FACS analysis of *Tel2*$^{DEL/FLOX}$ *p53*$^{-/-}$ MEFs expressing Tel2 or empty vector six days after H&R Cre retrovirus infection or mock infection. Mitotic cells were labeled with anti-histone H3 phospho-Serine 10 antibody and counter stained with PI to detect DNA content.

(B) FACS analysis of cell cycle profile. Indicated genotype of MEFs were used as controls for cells used in Fig. 2B. *Tel2*$^{FLOX/+}$*P53*$^{+/+}$ cells and *Tel2*$^{DEL/FLOX}$*p53*$^{-/-}$ expressing Tel2 cells were infected with the H&R Cre retrovirus or mock treated. Five or six days later, the cells were labeled with BrdU for 1hr, fixed, stained with FITC conjugated anti-BrdU antibody and counter stained with PI to detect DNA content.

Supplemental Figure 4

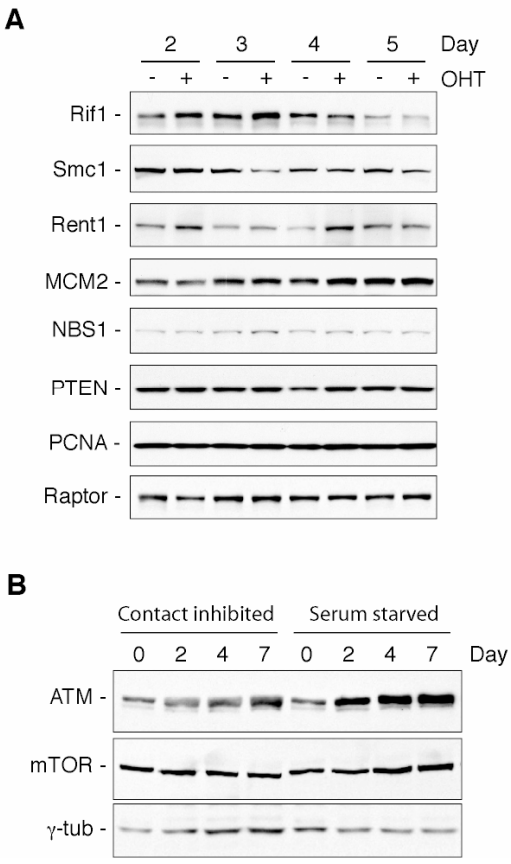

Figure S4. The effect of Tel2 deletion is specific for PIKKs and not explained from reduced entry into S phase.

(A) Cellular lysates prepared from SV40-LT transformed *Tel2*$^{DEL/FLOX}$ MEFs were used for Western blotting. The cells were treated with or without 0.5 μM OHT for 5 hr and harvested at the indicated time points after treatment. These samples were identical to those used in Fig. 4D.

(B) ATM and mTOR levels are not diminished in quiescent cells. Contact inhibited or serum starved BJ-TERT cells were harvested at indicated time points and analyzed by immunoblotting.

Supplemental Figure 5

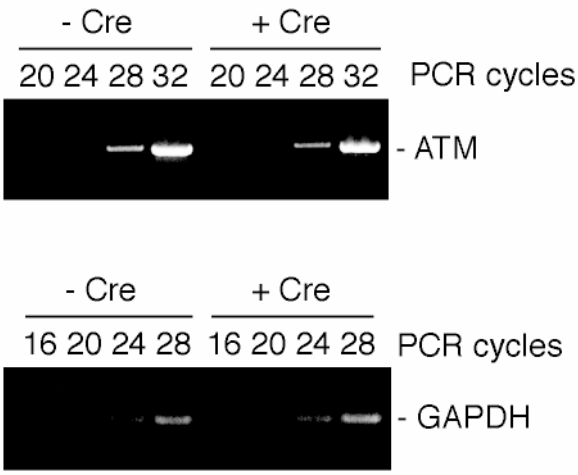

Figure S5. Tel2 gene deletion does not alter mRNA level of ATM.

ATM mRNA level examined by RT-PCR. SV40-LT transformed *Tel2*$^{DEL/FLOX}$ were infected with H&R Cre retrovorus and 4 days later the total RNA was extracted for the RT-PCR. As a control, the cells were treated similarly except for Cre retrovirus infection. GAPDH mRNA was amplified as loading control. PCR samples were analyzed at indicated PCR cycles.

Supplemental Figure 6 Takai et al.

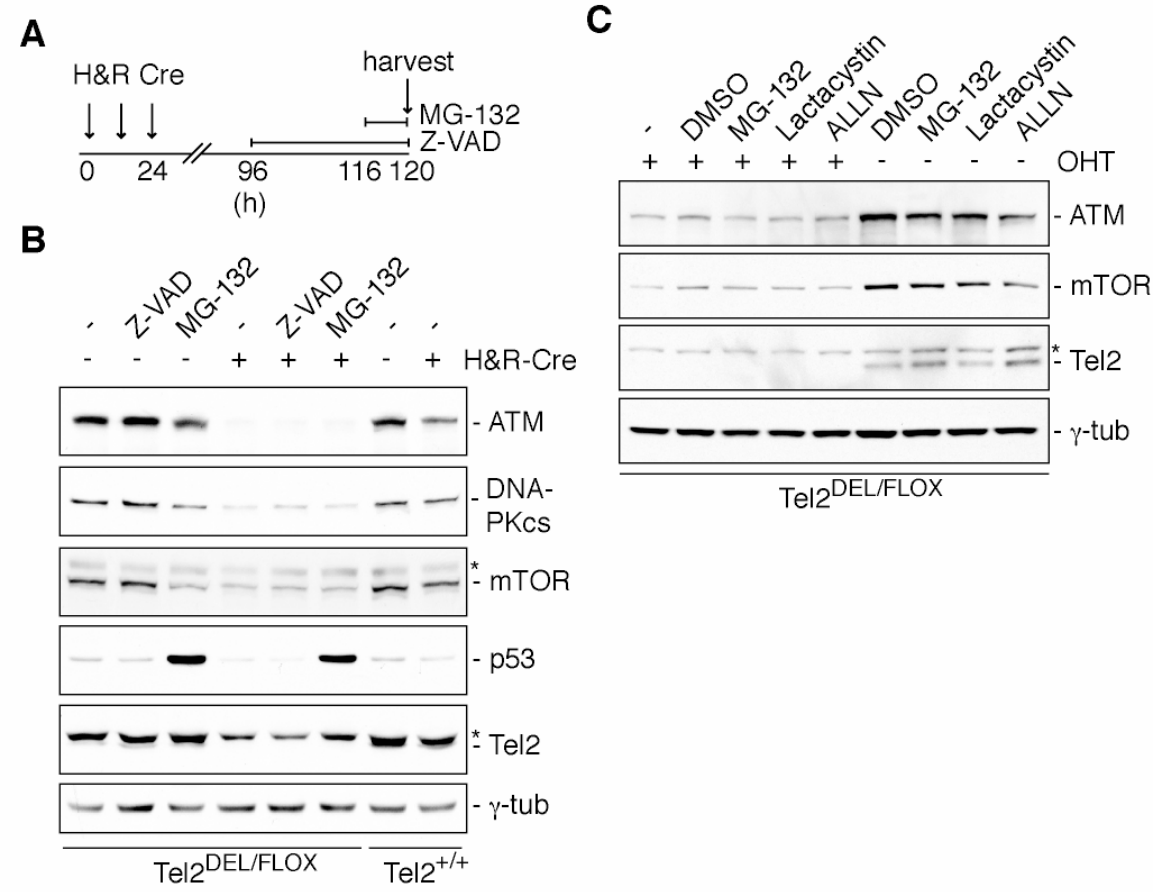

Figure S6. Effects of proteasome inhibitors on PIKKs.

(A) Experimental time line of the experiment shown in (B). Primary *Tel2*$^{DEL/FLOX}$*p53*$^{+/+}$ and *Tel2*$^{+/+}$ *p53*$^{+/+}$ MEFs were treated with or without H&R Cre, cultured for 96 hr or 116 hr before Z-VAD (Z-VAD(OME)-FMK, 627610, Chalbiochem) or MG-132 (474790 Calbiochem) treatment, respectively. Cells were treated with medium containing Z-VAD for 24 hr or MG-132 for 4 hr and harvested for Western blot analysis.

(B) Proteasome inhibition or caspase inhibition do not influence PIKK protein levels. The cells were treated with vehicle, 40 μM Z-VAD or 10 μM MG-132 as the time line indicated in (A) and harvested at day 5. Genotypes of the cells are as indicated. p53 protein was blotted as a positive control for the effect of MG-132. *, non-specific bands.

(C) Proteasome inhibitors do not alter ATM and mTOR protein levels. SV40-LT transformed *Tel2*$^{DEL/FLOX}$ MEFs were treated with 0.5 μM OHT for 4 hr to induce Tel2 depletion and cultured for an additional 60 hr. The cells were then treated either with

0.5% DMSO, 10 μM MG-132, 10 μM Lactacystin (426100, Calbiochem) or 20 μM ALLN (208750, Calbiochem) for 8 hr and harvested for Western blot analysis. As a control, the cells were treated similarly except for OHT treatment. *, non-specific band.

Supplemental Figure 7 Takai et al.

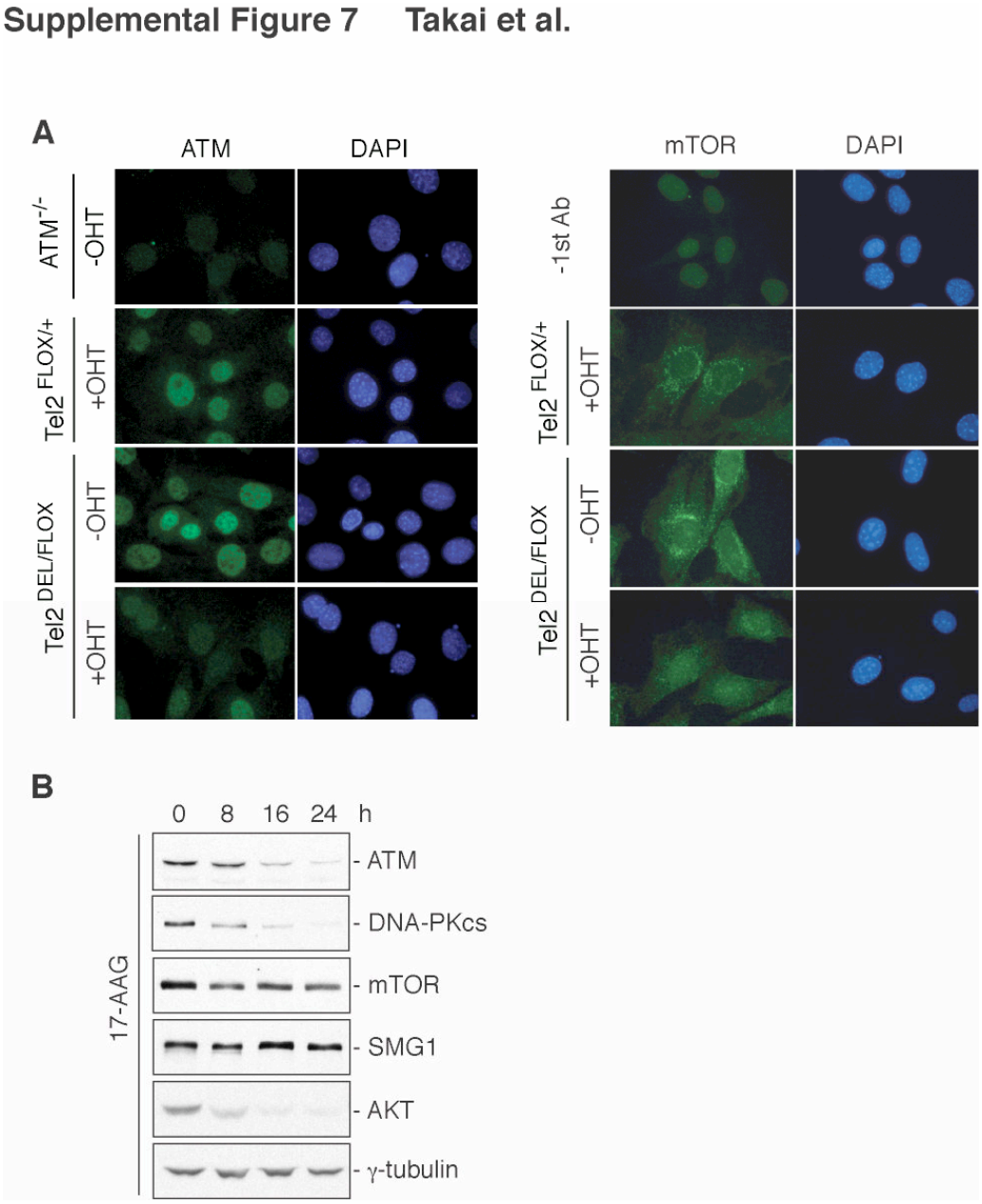

Figure S7. Localization of ATM and mTOR and effects of geldanamycin.

(A) Tel2 ablation does not result in altered localization of ATM or mTOR. Immunofluorescence for ATM (MAT3) or mTOR (#2972, Cell Signaling) (Alexa488, green) and DAPI stain for DNA (blue). SV40-LT transformed MEFs of indicated genotype were treated with or without 0.5 μM OHT, cultured for 3 days and fixed for

analysis. ATM$^{-/-}$ MEFs were used as a control of ATM detection. -1st Ab; MEFs were stained similarly except for the 1st antibody.

(B) Differential effect of the Hsp90 inhibitor 17-AAG on PIKKs. MEFs were treated with 1 μM 17-AAG (A8476, Sigma) for indicated periods and harvested for Western blot analysis. Vehicle treatment did not alter the protein levels analyzed (data not shown). AKT is shown as a positive control for the effect of 17-AAG.

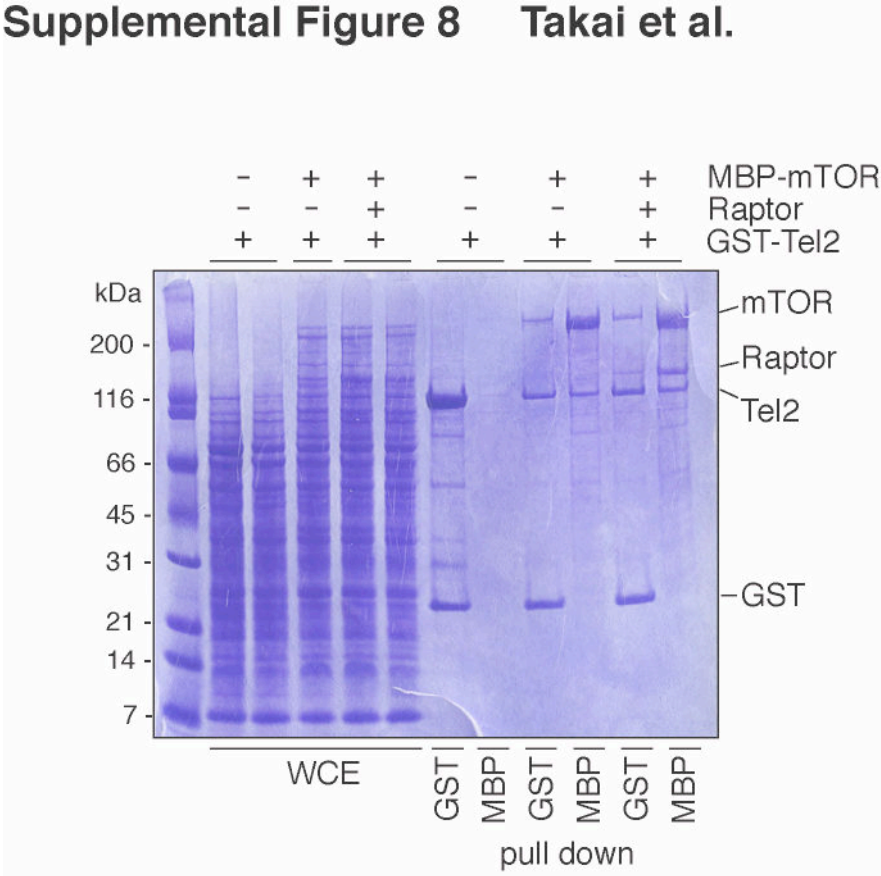

Figure S8. Interaction between Tel2 and mTOR with or without Raptor

Direct interaction between Tel2 and mTOR. Baculovirus derived GST-Tel2, MBP-mTOR and Raptor were co-expressed as indicated, affinity purified using affinity resins (indicated below the lanes), separated on SDS-PAGE, and visualized by CBB staining.